REPORT DOCUMENTATION PAGE

Form Approved
OMB NO. 0704-0188

1. AGENCY USE ONLY (Leave Blank)	2. REPORT DATE	3. REPORT TYPE AND DATES COVERED
	31st October 2007	Final 1st August 2004 - 31st July 2007

4. TITLE AND SUBTITLE
Development of multi-adaptive simulation technologies for nonlinear solid polymer viscoelasticity

5. FUNDING NUMBERS
ARO GRANT No. W911NF-04-1-0185

6. AUTHOR(S)
J.R. Whiteman, M.K. Warby, Simon Shaw

7. PERFORMING ORGANIZATION NAME(S) AND ADDRESS(ES)
BICOM, Brunel University, Uxbridge, Middlesex UB8 3PH, UK

8. PERFORMING ORGANIZATION REPORT NUMBER
CLOSEOUT, Y. 4

9. SPONSORING / MONITORING AGENCY NAME(S) AND ADDRESS(ES)
U. S. Army Research Office
P.O. Box 12211
Research Triangle Park, NC 27709-2211

10. SPONSORING / MONITORING AGENCY REPORT NUMBER
44434.3-EG

11. SUPPLEMENTARY NOTES
The views, opinions and/or findings contained in this report are those of the author(s) and should not be construed as an official Department of the Army position, policy or decision, unless so designated by other documentation.

12 a. DISTRIBUTION / AVAILABILITY STATEMENT
Approved for public release; Federal Purpose Rights

12 b. DISTRIBUTION CODE

13. ABSTRACT (Maximum 200 words)

This project has been concerned with the relaible computation of engineering Quantities of Interest (QoI), and the application of these mathematical methods to problems of interest to the US Army (informed by our long-standing contact with Dr A R Johnson, ARL, VTD, LaRC). In the project we have applied state-of-the-art mathematical theory to a practical large deformantion engineering problem in membrane inflation. In doing this we have applied modern methods of a posteriori error estimation in order to address the error in the engineering QoI that arise from modelling simplifications and also from finite element approximation. Our results show that this technique works in that it can be used to adaptively optimise the finite elenent mesh, as well as to give an indication of the physical error contained in the modelling assumptions.

The eventual benefit of research of this nature and the downstream uptake of the techniques and methodology into commercial engineering software cannot be overstated. By isolating and estimating the two principal sources of error in physical simulations (modelling and discretization) the software will allow the practitioner to assign a degree of confidence in the results that has never before been possible.

Close out report (funding period 1 April 2007 – 31 July 2007)

Development of multi-adaptive simulation technologies for nonlinear solid polymer viscoelasticity

J.R. Whiteman, M.K. Warby and Simon Shaw

BICOM and Math. Sciences, Brunel University, UB8 3PH, England
www.brunel.ac.uk/bicom

ARO Grant No.: **W911NF-04-1-0185**
ARO Proposal No.: **44434-EG**

Summary

Our research activity has been set in the context of a nonlinear finite deformation problem describing unsteady membrane inflation. We have developed theory and prototype software that is capable of estimating the errors in several physically relevant engineering QoI's. In the first part of the project these estimates were confined to only the finite element discretization error. In the last stages of the project we have been able to extend this error estimation to encompass the modelling error that results from neglecting the inertia term in Newton's second law of motion. Full details are given below; it is expected that these findings will appear in one or more journal publications.

In this project we have applied state-of-the-art mathematical theory to a practical engineering problem in membrane inflation. We have applied modern methods of *a posteriori* error estimation in order to address the error in engineering quantities of interest that arise from modelling simplifications and also from finite element approximation. Our results show that this technique works in that it can be used to adaptively optimise the finite element mesh, as well as give an indication of the physical error contained in the modelling assumptions.

The eventual benefit of research of this nature and the downstream uptake of the techniques and methodology into commercial engineering software cannot be overstated. By isolating and estimating the two principal sources of error in physical simulations (modelling and discretization) the software will allow the practitioner to assign a degree of confidence in the results that has never before been possible.

Contents

This is the close out report for the fourth funding period (1 April 2007 – 31 July 2007) as defined by the payment schedule of the contract.

1 Introduction

This project has been concerned with the reliable computation of engineering Quantities of Interest (QoI), and the application of these mathematical methods to problems of interest to the US Army (informed by our long-standing contact with Dr AR Johnson, ARL, VTD, LaRC).

Briefly, an engineer is often confronted with a difficult problem, the 'fine' problem, which in practical terms is an intractable computational task. Usually it is not every aspect of the solution that is of interest but only a certain quantity, the QoI. For example, this could be a localised stress, a mode shape or natural frequency, or even a measure of dissipated energy (damping).

To overcome the intractability it is routine to replace this fine problem with a 'coarse' problem which, it is judged, contains enough of the physics to reliably, but approximately, capture the QoI. This entails a *modelling error*. Furthermore, when this coarse problem is loaded in to finite element software the computed QoI then involves also a *discretization error*.

For some problems experienced engineering judgement alone may be enough to determine whether or not the computed QoI is accurate enough for the purpose of the application. However, sometimes the engineer's experience will suggest that the QoI may be computed inaccurately, or subtle effects in the problem may give rise to significant but unanticipated (and, possibly, undetected) errors in the QoI due to either or both of the modelling approximation or the finite element approximation.

Our research has focussed on the development of modern techniques in computational mathematics which afford a computational procedure for the 'black-box' estimation of both the modelling error and the discretization error in the computed QoI. This computed error estimate is then extra information that the engineer can make use of in determining whether or not the computer model is adequate at the level of need.

The basic idea behind this mathematical technique is to compute the solution to the coarse problem and place it into the fine problem's equations. The extent to which this solution does not satisfy the fine equations (the *residual*) gives a rough measure of how

adequate (or otherwise) the coarse solution is. However, this is a non-specific measure of 'adequacy'. To connect this residual to the engineer's specific QoI requires the additional computational step of determining a dual solution. This dual solution then multiplies the residual at every point in the finite element mesh and, by a prescribed procedure, these weighted residuals are summed up and the result is an estimate of the errors in the QoI.

This dual solution is not unlike the influence (or Green's) function from applied mathematics. Its value lies in the fact that a large residual, at a patch in the finite element mesh, may end up being weighted by a very small dual solution (over that patch). The net result is that, although the solution quality is low in that patch, the contribution to the error in the QoI is small, or even negligible. This information can then be used to provide a guide to local mesh and model refinement. And this, in turn, allows the engineer to tune the model and mesh to determine the QoI accurately with the minimum amount of computational effort on the coarse problem.

Of course, this extra functionality comes at a price – we can think of it as a tax on the cost of the coarse problem. The tax is levied on the extra information on the error and is manifest as the cost in computing the dual solution. We recognise that, in some applications, this tax is too high to bear but, in other applications, it can be seen as small relative to the overall cost of the engineering problem.

2 Dissemination activity at ARL, VTD, Langley

This is a summary of the trip to ARL, VTD, LaRC made by Whiteman, Shaw and Warby to visit with Dr AR Johnson during 9–15 October 2007.

The primary purpose of the trip was to disseminate findings from this ARO research project, and also to effect a technology transfer though discussion of our advanced applied engineering mathematics and by a transfer of our working computer software.

The secondary purpose of the trip was for us to understand current needs within ARL's broader mission, and to comment on how our research expertise might contribute toward that mission.

The next part of the report summarises our activities and conversations during our trip to ARL, and (where appropriate) attempts to sensibly comment on whether or not our technology may be able to make a practical contribution.

- **Seminar presentation:** Warby gave a seminar presentation of our research on October 10, 2007. The audience included Dr. AR Johnson as well as Drs. Bey and Tessler (NASA).
- **Code transfer:** Our working computer software was transferred to Dr. AR Johnson on October 13, 2007.
- **Theory transfer:** A detailed run through of the mathematics underlying the QoI error estimation technique was made with Dr. AR Johnson on October 13, 2007. It was noted that a comprehensive guide to this theory will be contained in this close out report to ARO.

- **Discussions with Dr RP Thornburgh:** We met with Dr Robert P Thornburgh on October 11, 2007. Dr Thornburgh explained the difficulties he has encountered in the reliable computation of the natural frequencies and mode shapes (the QoI's) of helicopters suffering inflight bending loads.

  1. He explained that such a small effect as modelling clamped boundary conditions as a continuous line, as opposed to a sequence of bolts, can throw off the computation of the QoI by a significant amount. Indeed, even variations in the diameter over which the bolts were clamped introduced a significant modelling error. This had non-trivial implications as to when and how apparently secondary structures such as cockpit glass and door panels should be included in the coarse model.
  2. Another significant difficulty arose in the modelling of the tail panels. Modelling the panel in each bay by a single finite element resulted in a computationally feasible problem but did not allow the (coarse) finite element model to predict panel buckling (through, for example, the introduction of surface imperfections). Adding enough elements to capture this effect, however, pushed the model into the computationally unfeasible domain.
  3. Dr. Thornburgh also introduced us to the current interest ARL has in uncertainty analysis and the work he had carried out with LTC Robert B Floersheim. We will comment further on this below and simply remark here that we hope, in due course, to obtain a copy of LTC Floersheim's thesis.

  We noted that while our technology could make a contribution in the first two areas, it is possible that the tax would be too high. Dr. Thornburgh's main requirement is that of obtaining an accurate QoI within reasonable time. The computation of the dual solution would, although giving estimates of the error in the QoI, introduce a significant time delay into the entire computational procedure.

  On the other hand, it is conceivable that our methodology could make a significant contribution in terms of uncertainty analysis (see below).

- **Discussions with Dr A Tessler (NASA):** On October 12, 2007, we discussed with Dr. Alex Tessler (NASA) his major contribution to zig-zag theory in the stress analysis of beam and plate structures. It is clear that such models can form a fine problem and that our QoI error estimation is relevant to this area.

- **Further discussions with Dr AR Johnson:** On October 12, 2007, we discussed with Dr. AR Johnson the Natick Soldier RDEC's ongoing work on air-supported structures. These structures are susceptible to significant ageing effects, geometric and material imperfections, large design tolerances, large deformations, and can be modelled by various mathematical techniques. In the context of **uncertainty analysis** it seems that our technology may be able to make a significant impact here. For example, assume that in-service conditions vary randomly about some mean (expected) values. The dual solution could be obtained just once on this state and then used to determine an optimal mesh as well as judge whether the modelling error in the QoI was at an acceptable level.

  Given this optimal mesh the air-supported structure could be simulated *efficiently* many thousands of times with randomly perturbed inputs. Each time a QoI would

be produced and from these outputs we could build its probability density function. This would be a valuable design tool in terms of when and how to select design tolerances and would inform quality control procedures in terms of variability of construction. Note that now the 'tax' is at the order of $1/1000$.

Although this project is now at a close we are, in terms of the above comments and observations, keeping in touch with Dr Johnson to further discuss the feasibility of seeking further ARO funding in order to contribute to the Army's needs.

3 The theoretical framework

In this section we outline the basic mathematical framework behind this error estimation technique. The presentation is deliberately 'abstract' so as to avoid giving specific details on the physical properties of the underlying problem. These details are given later.

The main idea behind modelling-error estimation is to consider a 'fine', or high fidelity, model which captures all the physics relevant to the problem, and a 'coarse' approximation which, we suppose, includes only those physical effects that are needed for the computer simulation. The issue then is to quantify the resulting 'modelling error'.

3.1 Abstract formulation: discussion

We consider the primal 'fine' problem: Find $U \in \mathcal{U}$ such that

$$A(U; v) = F(v) \quad \forall v \in V, \tag{3.1}$$

where $A : \mathcal{U} \times V \to \mathbb{R}$ is a semilinear form and $F : V \to \mathbb{R}$ is a linear functional. Typically, this is a variational form of a highly complex physical problem involving a nonlinear operator, A, and a sought solution, U.

Accepting that this is too computationally demanding to work with we introduce the following 'coarse' physical approximation to this problem as: find $u \in \mathcal{U}_0 \subset U$ such that,

$$A_0(u; v) = F_0(v) \quad \forall v \in V_0 \subset V, \tag{3.2}$$

where $A_0 : \mathcal{U}_0 \times V_0 \to \mathbb{R}$ is a semilinear form and $F_0 : V_0 \to \mathbb{R}$ is a linear functional. The resulting modelling error is then $U - u$.

For practical purposes we also need a computational formulation. This is: find $u_h \in \mathcal{U}_0^h \subset \mathcal{U}_0$ such that,

$$A_0(u_h; v) = F_0(v) \quad \forall v \in V_0^h. \tag{3.3}$$

This introduces a *discretization error*: $u - u_h$, and formed the subject of the first phase of this project.

Let $J : \mathcal{U} \to \mathbb{R}$ be a quantity of interest (QoI) then the total error in the computational model is,

$$J(U) - J(u_h) = \underbrace{J(U) - J(u)}_{\text{modelling error}} + \underbrace{J(u) - J(u_h)}_{\text{discretization error}}. \tag{3.4}$$

The bulk of this report is concerned with the modelling error term but for completeness we also include some material related to discretization error described in earlier reports as some of the description is independent of whether or not the error is due to modelling error or due to discretization error.

3.2 Abstract formulation: an outline of the procedure

In subsequent sections we describe in some detail various representations of $J(U) - J(u)$ that can be used to estimate this quantity without explicitly computing the fine solution U. In summary an outline involves the following.

1. We solve (3.3) to generate the coarse approximation $u_h \approx u \approx U$.
2. We then use u_h as data in what is called our dual problem which in the implementation described here involves the following: Find $z \in \mathcal{U}_0$ such that
$$A'(u_h; v, z) = J'(u_h; v) \quad \forall v \in \mathcal{U}_0, \tag{3.5}$$
where $A'(.;.,.)$ is the Gateaux derivative of $A(.;.)$ (see later for a definition) and where $\mathcal{U}_0$ is an appropriate space.
3. We then compute the right hand side in the estimate
$$J(U) - J(u) \approx F(z) - A(u_h; z). \tag{3.6}$$

In this way the form $A(.;.)$ describing the fine problem is needed to get the residual term in step 3 and also to describe the linear problem in step 2 but note that the only nonlinear problem that is solved is in generating u_h in step 1.

The above procedure partly fits the framework described in [3] with the main difference being that in this approach we use $A'(.;.,.)$ derived from $A(.;.)$ instead of some simpler approximation to it as is allowed in [3]. In this way we do about the best possible in the estimate in step 3 based upon only having u_h available with the cost of doing this being in the difficulty of setting-up and solving (3.5).

3.3 Abstract formulation detail: Introductory comments about the error $J(U) - J(u)$

In this section we give some expressions to approximate the difference $J(U) - J(u)$ in terms of a function z satisfying a derived problem (i.e. a dual problem) in each case. The approximating expression that we use is actually the same in each case and is of the form
$$J(U) - J(u) \approx F(z) - A(u; z) \tag{3.7}$$
with the difference between the cases being in how z is defined. The first derivations that we consider are useful when the approximate solution u is obtained using the same form $A(.;.)$ as is used to characterize the exact solution U, i.e. this is the case when we only have discretization error to consider. The problems involving z involves first Gateaux derivatives of $A(.;.)$ and of the QoI $J(.)$. For the derivation which is needed for the approximation which we use when we also have modelling error we additionally need higher Gateaux derivatives and thus these are described before the derivation is done.

3.4 Representations suitable when we only have discretization error

Let V be a function space, let $J : V \to \mathbb{R}$ be a functional and let $U \in V$ and $u \in V$ be functions. Also let $e_u = U - u$. The representations described here are partly derived by just using the fundamental theorem of calculus as follows. We let

$$g : [0,1] \to \mathbb{R}, \quad g(s) = J(u + se_u) \tag{3.8}$$

so that

$$J(U) - J(u) = g(1) - g(0) = \int_0^1 g'(s)\,\mathrm{d}s. \tag{3.9}$$

This leads us to introduce first Gateaux derivatives of functionals which are defined by

$$J'(u;v) := \lim_{s\to 0} \frac{J(u+sv) - J(u)}{s} = \frac{\mathrm{d}}{\mathrm{d}s} J(u+sv)\bigg|_{s=0} \tag{3.10}$$

so that with this notation we have

$$J(U) - J(u) = \int_0^1 J'(u + se_u; e_u)\,\mathrm{d}s. \tag{3.11}$$

We similarly define a Gateaux derivative of $A(.;.)$ by

$$A'(u;v,w) = \frac{\mathrm{d}}{\mathrm{d}s} A(u+sv;w)\bigg|_{s=0} \tag{3.12}$$

and thus we similarly have

$$A(U;w) - A(u;w) = \int_0^1 A'(u + se_u; e_u, w)\,\mathrm{d}s. \tag{3.13}$$

In (3.11) and (3.13) we have differentiation in the direction of the error e_u which in the applications is unknown. To proceed further we consider differentiation in all possible directions v and seek a function $z \in V$ such that

$$\int_0^1 A'(u + se_u; v, z)\,\mathrm{d}s = \int_0^1 J'(u + se_u; v)\,\mathrm{d}s \quad \text{for all } v \in V. \tag{3.14}$$

If we can obtain such a function z then, with $v = e_u$, we have the representation

$$J(U) - J(u) = A(U;z) - A(u;z) = F(z) - A(u;z). \tag{3.15}$$

The representation (3.15) with z defined in (3.14) cannot be used in the computations as given because the equation for z depends on the exact solution U as the integral involves a path from u (when $s = 0$) to U (when $s = 1$). To get something which can be used in computations we must replace (3.14) by something which only involves terms which can be computed. As it is assumed here that we can obtain u, the simplest approximation is to use a one point quadrature on the integral involving evaluation only at $s = 0$ giving

$$A'(u;v,z) = J'(u;v) \quad \text{for all } v \in V \tag{3.16}$$

with now for this $z \in V$

$$J(U) - J(u) \approx F(z) - A(u;z). \tag{3.17}$$

In situations when we can obtain an estimate $\hat{e}_u \approx e_u$ we can do a bit better by approximating (3.14) by replacing the unknown e_u by $\hat{e}_u$ and then approximating each integral by the trapezoidal rule to give the problem of finding $z \in \hat{V}_h$, where $\hat{V}_h$ is a finite dimensional space, such that

$$\begin{aligned} A'(u+\hat{e}_u; v, z) + A'(u; v, z) &= J'(u+\hat{e}_u; v) + J'(u; v) \quad \text{for all } v \in \hat{V}_h. && (3.18) \\ J(U) - J(u) &\approx F(z) - A(u; z) && (3.19) \end{aligned}$$

In practical situations when there is only discretization error to consider this works well provided a suitable $\hat{e}_u \approx e_u$ can be obtained and provided the function z obtained from (3.18) is sufficiently close to the function z satisfying (3.14). Observe that if $u \in V_h$ satisfies $A(u; v) = F(v)$ for all $v \in V_h$ then we must seek z from a larger space than V_h as otherwise our estimate of $J(U) - J(u)$ would just be 0. We comment on this further in subsection 3.7.

3.5 The definition of Gateaux derivatives again and Taylor's series

As indicated above, Gateaux derivatives are concerned with differentiating forms and functionals in the direction of functions. Specifically, with V denoting a function space we have, repeating the definitions above, that

$$\begin{aligned} J'(u; v) &:= \lim_{s\to 0} \frac{J(u+sv) - J(u)}{s} = \frac{\mathrm{d}}{\mathrm{d}s} J(u+sv)\Big|_{s=0}, && (3.20) \\ A'(u; v, w) &:= \lim_{s\to 0} \frac{A(u+sv; w) - A(u; w)}{s} = \frac{\mathrm{d}}{\mathrm{d}s} A(u+sv; w)\Big|_{s=0}. && (3.21) \end{aligned}$$

The semi-colons in both cases indicate that the terms are possibly non-linear in the terms to the left of the semi-colon and are linear in the terms to the right of the semi-colon. In the case of $A'(u; v, w)$ the derivative is respect to the term just to the right of the semi-colon (i.e. v). It should be noted here that in general if we swap v and w we get a different number although when quasi-static problems are described we will have situations in which we have terms which are symmetric in v and w.

By differentiating these first derivatives in a similar way we get second Gateaux derivatives and we can continue this to define higher derivatives, i.e.

$$\begin{aligned} J''(u; v_1, v_2) &:= \frac{\mathrm{d}}{\mathrm{d}s} J'(u+sv_1; v_2)\Big|_{s=0}, && (3.22) \\ J'''(u; v_1, v_2, v_3) &:= \frac{\mathrm{d}}{\mathrm{d}s} J''(u+sv_1; v_2, v_3)\Big|_{s=0}, && (3.23) \\ &\text{etc.} && (3.24) \end{aligned}$$

In terms of these higher derivatives we can write Taylor's series as

$$\begin{aligned} g(s) = J(u+sv) &= g(0) + sg'(0) + \frac{s^2}{2} g''(0) + \frac{s^3}{6} g'''(0) + \cdots && (3.25) \\ &= J(u) + J'(u; sv) + \frac{1}{2} J''(u; sv, sv) + \frac{1}{6} J'''(u; sv, sv, sv) + \cdots && (3.26) \end{aligned}$$

3.6 Preliminaries: Taylor's series in $\mathbb{R}$ with remainder, the Peano Kernel representation and the Trapezoidal rule

Before we consider another representation for $J(U) - J(u)$ we need a result concerning the error in the trapezoidal rule which we can obtain as follows.

First let $x, t \in \mathbb{R}$ and let

$$(x-t)_+^n := \begin{cases} (x-t)^n, & \text{if } x-t > 0, \\ 0, & \text{otherwise.} \end{cases} \tag{3.27}$$

Then to obtain Taylor's series with the remainder in integral form for a function which is $n+1$-times continuously differentiable we consider, for $0 \leq x \leq 1$, the following term which we re-express using integration by parts repeatedly.

$$\begin{aligned} R_n &= \frac{1}{n!}\int_0^1 (x-t)_+^n f^{(n+1)}(t)\,\mathrm{d}t = \frac{1}{n!}\int_0^x (x-t)^n f^{(n+1)}(t)\,\mathrm{d}t & (3.28)\\ &= R_{n-1} + \frac{1}{n!}\Big[(x-t)^n f^{(n)}(t)\Big]_0^x = R_{n-1} - \frac{1}{n!}x^n f^{(n)}(0), \quad \text{by parts,} & (3.29)\\ &= \cdots = R_0 - \sum_{k=1}^{n}\frac{1}{k!}x^k f^{(k)}(0), \quad \text{by induction.} & (3.30) \end{aligned}$$

Now since

$$R_0 = \int_0^x f^{(1)}(t)\,\mathrm{d}t = f(x) - f(0) \tag{3.31}$$

we obtain the result

$$f(x) = \sum_{k=0}^{n}\frac{1}{k!}x^k f^{(k)}(0) + R_n. \tag{3.32}$$

Next, if L is a linear functional for which we can interchange the $L(.)$ operation and the integral operation over $[0,1]$ then we have

$$L(f) = \sum_{k=0}^{n}\frac{1}{k!}L(x^k)f^{(k)}(0) + \frac{1}{n!}\int_0^1 L((x-t)_+^n)f^{(n+1)}(t)\,\mathrm{d}t, \tag{3.33}$$

where in the integral the $L(.)$ operation is being done on a function of x. This representation is particularly useful when the operator $L(.)$ is such that $L(x^k) = 0$ for $k = 0, 1, \cdots, n$ as then the representation reduces to

$$L(f) = \frac{1}{n!}\int_0^1 L((x-t)_+^n)f^{(n+1)}(t)\,\mathrm{d}t. \tag{3.34}$$

This is known as the Peano kernel representation of $L(f)$.

We now apply the Peano kernel representation to the following operator L given by

$$L(f) := \int_0^1 f(x)\,\mathrm{d}x - \frac{f(0)+f(1)}{2}. \tag{3.35}$$

which gives the error in the trapezoidal rule. We have $L(1) = L(x) = 0$ but $L(x^2) \neq 0$ and thus in the Peano Kernel result we have $n = 1$. With $0 \leq t \leq 1$, the integrand gives

$$\begin{aligned} L((x-t)_+) &= \int_0^1 (x-t)_+\,\mathrm{d}x - \left(\frac{1-t}{2}\right)\\ &= \int_t^1 (x-t)\,\mathrm{d}x - \left(\frac{1-t}{2}\right) = \frac{1}{2}\left((1-t)^2 - (1-t)\right) = \frac{1}{2}(t-1)t. \end{aligned}$$

Thus

$$L(f) := \int_0^1 f(x)\,\mathrm{d}x - \frac{f(0)+f(1)}{2} = \frac{1}{2}\int_0^1 f^{(2)}(t)(t-1)t\,\mathrm{d}t. \tag{3.36}$$

3.7 Further comments about the order of magnitude of $J(U) - J(u)$ and the accuracy needed in the approximation of z

With the preliminaries of the previous subsections it is now convenient to return briefly to the versions of z considered in subsection 3.4. Firstly, suppose that z is defined by (3.14) giving the exact representation (3.15) and the set-up is such that $U \in V$ and $u \in V_h \subset V$ is of the form $u = u_h = U - e_u$, (where h indicates the mesh size) and satisfies

$$A(u_h; v) = F(v) \quad \text{for all } v \in V_h. \tag{3.37}$$

In this case $J(U) - J(u_h)$ is zero if $U = u_h$ and is also zero if $z \in V_h$. These two different cases when $J(U) - J(u)$ is 0 enables us to deduce something about the magnitude of this term. Mathematically then for any $z_h \in V_h$ we have

$$\begin{aligned}
J(U) - J(u_h) &= F(z) - A(u_h; z) && (3.38)\\
&= F(z) - A(u_h; z) - (F(z_h) - A(u_h; z_h)) && (3.39)\\
&= F(z - z_h) - A(u_h; z - z_h) && (3.40)\\
&= F(z - z_h) - A(U - e_u; z - z_h) && (3.41)\\
&= F(z - z_h) - A(U; z - z_h) + A'(U; e_u, z - z_h) + \cdots && (3.42)\\
&= A'(U; e_u, z - z_h) + \cdots . && (3.43)
\end{aligned}$$

With $A'(.;.,.)$ being linear in terms after the semi-colon this tells us that the magnitude of $J(U) - J(u_h)$ depends on the product of the magnitudes of e_u and $z - z_h$. Thus in situations when the QoI functional $J(.)$ is such that the function z is sufficiently smooth we have typically that the quantities e_u and $z - z_h$ are $\mathcal{O}(h^p)$ in magnitude, where p depends on the degree of the piecewise polynomials used, and $J(U) - J(u_h)$ is $\mathcal{O}(h^{2p})$. That is, we are likely to approximate the QoI more accurately than we approximate U.

The function z defined in (3.14), which we are not likely to be able to compute, is the not the same as the function z defined in (3.18) which involves $\hat{e}_u$ instead of e_u, a finite dimensional space $\hat{V}_h$ and the trapezoidal rule approximation of the integral. To distinguish between these functions let $z \in V$, $\bar{z}_h \in V$, $\tilde{z}_h \in \bar{V}_h$, and $\hat{z}_h \in \bar{V}_h$ satisfy respectively

$$\begin{aligned}
\int_0^1 A'(u + se_u; v, z)\,\mathrm{d}s &= \int_0^1 J'(u + se_u; v)\,\mathrm{d}s \quad \text{for all } v \in V, && (3.44)\\
\int_0^1 A'(u + s\hat{e}_u; v, \bar{z}_h)\,\mathrm{d}s &= \int_0^1 J'(u + s\hat{e}_u; v)\,\mathrm{d}s \quad \text{for all } v \in V, && (3.45)\\
\int_0^1 A'(u + s\hat{e}_u; v, \tilde{z}_h)\,\mathrm{d}s &= \int_0^1 J'(u + s\hat{e}_u; v)\,\mathrm{d}s \quad \text{for all } v \in \hat{V}_h, && (3.46)\\
A'(u + \hat{e}_u; v, \hat{z}_h) + A'(u; v, \hat{z}_h) &= J'(u + \hat{e}_u; v) + J'(u; v) \quad \text{for all } v \in \hat{V}_h. && (3.47)
\end{aligned}$$

The function $\hat{z}_h$ is what we actually compute.

We next compare z, $\bar{z}_h$, $\tilde{z}_h$ and $\hat{z}_h$ and comment on the properties that we need from $\hat{e}_u$ and $\hat{V}_h$ to produce a sufficiently good estimate $\hat{z}_h \approx z$ for the purpose of the error estimate. In the reasoning we assume throughout that u and U are not too close to critical points such as limit points and bifurcation points so that the linear problems (3.44)–(3.47) have unique solutions which are not too sensitive to changes in the data. We will also assume that $\|e_u\|$ is $\mathcal{O}(h^p)$. For the estimate of the error we will assume that this can be done by constructing $\hat{e}_u$ so that $\|e_u - \hat{e}_u\| = \mathcal{O}(h^{p+1})$. In such a case there is only a change of $\mathcal{O}(h^{p+1})$ in the data from (3.44) to (3.45) and thus $\|z - \bar{z}_h\| = \mathcal{O}(h^{p+1})$. To have a similar change when we compare (3.45) and (3.46) requires that $\hat{V}_h$ is sufficiently large that this is the approximating power of this space. That is, if we get $\mathcal{O}(h^p)$ approximations using the space V_h then we need $\hat{V}_h \supset V_h$ to contain polynomials of one degree higher to have an approximating capability of $\mathcal{O}(h^{p+1})$. When this is the case we have $\|\bar{z}_h - \tilde{z}_h\| = \mathcal{O}(h^{p+1})$. Finally, to compare (3.46) and (3.47) we note that by using (3.36) we have

$$\begin{aligned}
&\int_0^1 J'(u + s\hat{e}_u; v)\,\mathrm{d}s - \frac{1}{2}(J'(u + \hat{e}_u; v) + J'(u; v)) \\
&= \frac{1}{2}\int_0^1 J'''(u + s\hat{e}_u; \hat{e}_u, \hat{e}_u, v)s(s-1)\,\mathrm{d}s \qquad (3.48)\\
&\int_0^1 A'(u + s\hat{e}_u; v, \tilde{z})\,\mathrm{d}s - \frac{1}{2}(A'(u + \hat{e}_u; v, \tilde{z}) + A'(u; v, \tilde{z})) \\
&= \frac{1}{2}\int_0^1 A'''(u + s\hat{e}_u; \hat{e}_u, \hat{e}_u, v, \tilde{z})s(s-1)\,\mathrm{d}s. \qquad (3.49)
\end{aligned}$$

With $\|e_u\|$ being $\mathcal{O}(h^p)$ and the integrands involving products of such terms, the trapezoidal rule approximation only changes the data by $\mathcal{O}(h^{2p})$ and we have $\|\tilde{z}_h - \hat{z}_h\| = \mathcal{O}(h^{2p})$. Combining all these comparisons gives us that $\|z - \hat{z}_h\|$ is $\mathcal{O}(h^{p+1})$. As a consequence, when we compare

$$J(U) - J(u) = F(z) - A(u; z) \quad \text{with} \quad F(\hat{z}_h) - A(u; \hat{z}_h) \qquad (3.50)$$

we have, similar to the derivation (3.38)–(3.43), that

$$\begin{aligned}
& F(z) - A(u; z) - (F(\hat{z}_h) - A(u; \hat{z}_h)) && (3.51)\\
= \;& F(z - \hat{z}_h) - A(u; z - \hat{z}_h) && (3.52)\\
= \;& F(z - \hat{z}_h) - A(U - e_u; z - \hat{z}_h) && (3.53)\\
= \;& F(z - \hat{z}_h) - A(U; z - \hat{z}_h) + A'(U; e_u, z - \hat{z}_h) + \cdots && (3.54)\\
= \;& A'(U; e_u, z - \hat{z}_h) + \cdots && (3.55)
\end{aligned}$$

With $\|e_u\|$ being $\mathcal{O}(h^p)$ and $\|z - \hat{z}_h\|$ being $\mathcal{O}(h^{p+1})$ the error in the estimate using $\hat{z}_h$ is $\mathcal{O}(h^{2p+1})$ in magnitude which gives us asymptotic exactness as $J(U) - J(u)$ is $\mathcal{O}(h^{2p})$.

The asymptotic exactness just described relied on $\hat{e}_u$ being such that $\|e_u - \hat{e}_u\| = \mathcal{O}(h^{p+1})$ and that $\hat{V}_h$ being such that $\|\bar{z}_h - \tilde{z}_h\| = \mathcal{O}(h^{p+1})$. We can relax these requirements at the expense of reducing to a consistent estimate of $J(U) - J(u)$ if it is possible to compute $\hat{e}_u$ such that $\|e_u - \hat{e}_u\| \leq c_1\|e_u\|$, where c_1 is a constant satisfying $0 \leq c_1 < 1$, and $\hat{V}_h \supset V_h$ is sufficiently larger than V_h to generate a sufficiently better approximation than would be obtained if only V_h is used.

3.8 Remarks about when critical points occur

The above assumes that we are not close to critical points and thus to complete these comments we remark as to how such points are characterised in this abstract setting. Now in what has been given so far we have that $U \in V$ satisfies

$$A(U; v) = F(v) \quad \text{for all } v \in V. \tag{3.56}$$

In the application described in this report this brief notation hides some of the detail as in the quasi-static problem to be considered the function U represents a displacement field at time t as a result of a loading $P(t)$. That is we have the situation

$$A(U(t), P(t); v) = F(v) \quad \text{for all } v \in V. \tag{3.57}$$

(In our application $F(.)$ does not vary with t.) Now if we consider an increment of time Δt and let $\Delta U = U(t + \Delta t) - U(t)$ then at time $t + \Delta t$ we have

$$\begin{aligned} F(v) &= A(U(t + \Delta t), P(t + \Delta t); v) && (3.58)\\ &= A(U(t), P(t + \Delta t); v) + A'(U(t), P(t + \Delta t); \Delta U, v) + \cdots && (3.59)\\ &= \left(A(U(t), P(t); v) + \Delta t \frac{\partial P}{\partial t} \frac{\partial}{\partial t} A(U(t), P(t); v) + \cdots \right) && (3.60)\\ &\quad + A'(U(t), P(t); \Delta U, v) + \cdots && (3.61) \end{aligned}$$

By using (3.57), dividing by Δt and letting $\Delta t \to 0$ gives

$$A'(U(t), P(t); \frac{\partial U}{\partial t}, v) = -\frac{\partial P}{\partial t} \frac{\partial}{\partial t} A(U(t), P(t); v) \quad \text{for all } v \in V \tag{3.62}$$

which is an equation for the velocity $\frac{\partial U}{\partial t}$. If at some time t_c the form $A'(U(t_c), P(t_c); ., .)$ is such that there exists a function $w \in V$, $w \neq 0$ with

$$A'(U(t_c), P(t_c); \psi, w) = 0 \quad \text{for all } \psi \in V \tag{3.63}$$

then we have what is known as a critical point. In such a case we do not have a unique solution of a dual problem such as (3.16) since if z is a solution then $z + \beta w$ is also a solution for all $\beta \in \mathbb{R}$. When we are at such a point, letting $v = w$ in (3.62) gives

$$\frac{\partial P}{\partial t}(t_c) \frac{\partial}{\partial t} A(U(t_c), P(t_c); w) = 0 \tag{3.64}$$

and one or both of the terms in the product must be 0. The limit point case corresponds to when

$$\frac{\partial P}{\partial t}(t_c) = 0 \tag{3.65}$$

and thus if the loading has been such that $\frac{\partial P}{\partial t} > 0$ for $0 \leq t < t_c$, i.e. the loading has been increasing, then it becomes necessary to decrease the loading for t near t_c with $t > t_c$ in order to follow the solution path. This will not be pursued here with the purpose of these comments being just to indicate that the techniques of representing the error $J(U) - J(u)$ in terms of a dual solution z breaks down when critical points are encountered.

3.9 A general expression for $J(U) - J(u)$ when we have modelling error

We now consider the difference $J(U)-J(u)$ again without specifying how the approximate solution u is obtained or how the function z is obtained and as such it is suitable in cases where we may solve a different problem to generate them, i.e. we have modelling error. The representation given here is similarly derived in [3] and see also [2] which contains similar results.

As before, let $F(v)$ be a linear functional defined on a space V and suppose that U satisfies the following

$$A(U; v) = F(v), \quad \text{for all } v \in V. \tag{3.66}$$

Related to (3.66) we also suppose that $Z \in V$ satisfies

$$A'(U; v, Z) = J'(U; v), \quad \text{for all } v \in V. \tag{3.67}$$

As before $u \approx U$ and we let $z \approx Z$ be obtained in some way and let the errors in these approximations be defined by

$$e_u = U - u \quad \text{and} \quad e_z = Z - z. \tag{3.68}$$

Let

$$\begin{aligned} g_0(s) &= J(u + se_u) + F(z + se_z) - A(u + se_u; z + se_z), & (3.69)\\ g_1(s) &= J'(u + se_u; e_u) - A'(u + se_u; e_u, z + se_z), & (3.70) \end{aligned}$$

and observe that

$$g_0(1) = J(U), \quad g_0(0) = J(u) + F(z) - A(u; z), \quad g_1(1) = 0. \tag{3.71}$$

Thus

$$J(U) - J(u) = g_0(1) - g_0(0) + F(z) - A(u; z). \tag{3.72}$$

Now by the trapezoidal rule with remainder we have

$$g_0(1) - g_0(0) = \int_0^1 g_0'(s)\,\mathrm{d}s = \frac{1}{2}(g_0'(0) + g_0'(1)) + \frac{1}{2}\int_0^1 s(s-1)g_0'''(s)\,\mathrm{d}s. \tag{3.73}$$

For the derivative of g_0 we have

$$\begin{aligned} g_0'(s) &= J'(u + se_u; e_u) + F(e_z) - A'(u + se_u; e_u, z + se_z) - A(u + se_u; e_z) & (3.74)\\ &= g_1(s) + F(e_z) - A(u + se_u; e_z). & (3.75) \end{aligned}$$

Thus

$$g_0'(1) = 0, \quad g_0'(0) = g_1(0) + F(e_z) - A(u; e_z) \tag{3.76}$$

and we have

$$\begin{aligned} g_0(1) - g_0(0) &= \frac{1}{2}\left(g_0'(0) + \int_0^1 s(s-1)g_0'''(s)\,\mathrm{d}s\right) & (3.77)\\ &= \frac{1}{2}\left(g_1(0) + F(e_z) - A(u; e_z) + \int_0^1 s(s-1)g_0'''(s)\;\mathrm{d}s\right). & (3.78) \end{aligned}$$

As $g_1(1) = 0$ we have

$$g_1(0) = -\int_0^1 g_1'(s)\ \mathrm{d}s \tag{3.79}$$

$$= -\int_0^1 (J''(u+se_u;e_u,e_u) - A''(u+se_u;e_u,e_u,z+se_z) - A'(u+se_u;e_u,e_z))\ \mathrm{d}s \tag{3.80}$$

$$= -\int_0^1 (J''(u+se_u;e_u,e_u) - A''(u+se_u;e_u,e_u,z+se_z))\ \mathrm{d}s + (A(U;e_z) - A(u;e_z)). \tag{3.81}$$

Combining (3.78) and (3.81) and noting that $F(e_z) = A(U;e_z)$ gives

$$g_0(1) - g_0(0) = F(e_z) - A(u;e_z)$$
$$+\frac{1}{2}\left(\int_0^1 A''(u+se_u;e_u,e_u,z+se_u) - J''(u+se_u;e_u,e_u) + s(s-1)g_0'''(s)\ \mathrm{d}s\right).$$

Finally combining with (3.72) gives

$$J(U) - J(u) = (F(z) - A(u;z)) + (F(e_z) - A(u;e_z)) + \text{smaller terms.} \tag{3.82}$$

Again this is back to the estimate

$$J(U) - J(u) \approx F(z) - A(u;z) \tag{3.83}$$

and the simplest approximation z that we can obtain assuming that only u is available is to take the function z satisfying

$$A'(u;v,z) = J'(u;v) \quad \text{for all } v \in V. \tag{3.84}$$

4 The physical problem: Application of the theory to membrane inflation

In this section we consider the physical models in which we are going to apply the theory of representing the error in a QoI. Specifically, we consider the equations describing the inflation of a hyperelastic membrane. With $\underline{U}$ denoting the exact displacement and $\underline{V}$ denoting the exact velocity the weak forms will be written in the form

$$A(\begin{pmatrix}\underline{U}\\ \underline{V}\end{pmatrix};\begin{pmatrix}\underline{\psi}\\ \underline{\theta}\end{pmatrix}) = F(\begin{pmatrix}\underline{\psi}\\ \underline{\theta}\end{pmatrix}) \quad \text{for all appropriate } \underline{\psi} \text{ and } \underline{\theta} \tag{4.1}$$

in the dynamic case and in the form

$$a(\underline{U};\underline{\psi}) = F(\underline{\psi}) \quad \text{for all appropriate } \underline{\psi}, \tag{4.2}$$

at each time t, in the quasi-static case. In this latter case the form $a(\underline{U};\underline{\psi})$ is sometimes also written as $a(\underline{U};\underline{\psi})_\Omega$, when we wish to explicitly show the domain involved, and can also be written as $a(\underline{U},P(t);\underline{\psi})_\Omega$, when we also wish to explicitly indicate that the form depends on a loading term $P(t)$ at time t.

4.1 The inflation of an elastic membrane

We assume that the reference region of the body being deformed is given by

$$\Omega_{3D} = \{(X_1, X_2, X_3) : \quad (X_1, X_2) \in \Omega, \quad |X_3| < h_0/2\} \tag{4.3}$$

and we are considering the deformation over a time interval

$$0 \leq t \leq T. \tag{4.4}$$

The components X_1, X_2 and X_3 are with respect to a fixed cartesian coordinate system. We suppose that $|h_0|$ is small as part of a membrane idealization of how the sheet deforms. In the axi-symmetric case Ω is a circle and if the circle has radius 1 then we can take $\Omega = (0,1) = \{0 < r < 1\}$ with respect to cylindrical polar coordinates r, ψ, x_3. Here Ω is the region of the undeformed mid-surface.

The deformation of the body is described by the mapping

$$\underline{X} \to \underline{x} := \underline{X} + \underline{U}, \tag{4.5}$$

where $\underline{x} = \underline{x}(\underline{X}, t)$ is the deformed position and $\underline{u}(\underline{X}, t)$ is the displacement. The deformation gradient $\mathbf{F}_{3D}$ (which is the Jacobian of this mapping) is given by

$$\mathbf{F}_{3D} = \mathbf{I}_{3D} + \nabla_{3D}\underline{U}, \quad \text{where } \nabla_{3D}\underline{U} = \left(\frac{\partial \underline{U}}{\partial X_1}, \frac{\partial \underline{U}}{\partial X_2}, \frac{\partial \underline{U}}{\partial X_3}\right). \tag{4.6}$$

Here $\mathbf{I}_{3D}$ is the identity tensor. Note that in terms of components $\mathbf{F}_{3D}$ and $\nabla_{3D}\underline{U}$ are represented by 3×3 matrices. For our membrane model we use the notation $\mathbf{F}$ and $\nabla \underline{U}$ for the corresponding 3×2 quantities

$$\mathbf{F} = \begin{pmatrix} F_{11} & F_{12} \\ F_{21} & F_{22} \\ F_{31} & F_{32} \end{pmatrix} \quad \text{and} \quad \nabla \underline{U} = \left(\frac{\partial \underline{U}}{\partial X_1}, \frac{\partial \underline{U}}{\partial X_2}\right). \tag{4.7}$$

We restrict consideration to incompressible materials which means that

$$\det \mathbf{F}_{3D} = 1, \quad \text{and the density } \rho = \text{const.} \tag{4.8}$$

The simplifications to this when we have an axi-symmetric problem and we use cylindrical polars is that the deformation of the mid-surface is given by

$$(r, \psi, 0) \to (r + U_1, \psi, U_3) \quad \text{giving} \quad \mathbf{F} = \begin{pmatrix} 1 + U_1' & 0 \\ 0 & 1 + \frac{U_1}{r} \\ U_3' & 0 \end{pmatrix} \tag{4.9}$$

with $'$ denoting differentiation with respect to r.

Let $\boldsymbol{\sigma}$ denote the Cauchy stress tensor and let

$$\boldsymbol{\Pi}_{3D} = (\det \mathbf{F}_{3D})\mathbf{F}_{3D}^{-1}\boldsymbol{\sigma} = \mathbf{F}_{3D}^{-1}\boldsymbol{\sigma} \tag{4.10}$$

denote the nominal stress tensor. Let $\underline{n}$ denote the unit normal to the deformed mid-surface. This direction corresponds to the x_3-direction in the reference configuration. In the membrane approximation of how a thin sheet deforms it is assumed that $\sigma \underline{n} = \underline{0}$ which

corresponds to the fact that the stress components corresponding to the direction $\underline{n}$ in an actual thin sheet are generally much smaller in magnitude as compared to the tangential components. This in turn implies that the third column of $\mathbf{\Pi}_{3D}^T$ is $\underline{0}$ with respect to cartesian coordinates and as a consequence the membrane first Piola stress can be taken as

$$\mathbf{\Pi}^T = \begin{pmatrix} \Pi_{11} & \Pi_{21} \\ \Pi_{12} & \Pi_{22} \\ \Pi_{13} & \Pi_{23} \end{pmatrix} \tag{4.11}$$

and we have

$$\mathbf{\Pi}_{3D} : \nabla_{3D}\underline{\psi} = \mathbf{\Pi} : \nabla\underline{\psi}, \tag{4.12}$$

where here : denotes the double dot product operation, i.e. $\mathbf{A} : \mathbf{B} = \sum_{ij} A_{ij}B_{ij} = \text{tr}(\mathbf{A}^T\mathbf{B})$. With this result and when $|h_0|$ is small we have

$$\int_{\Omega_{3D}} \mathbf{\Pi}_{3D}^T : \nabla_{3D}\underline{\psi}\ \mathrm{d}\underline{X} \approx h_0 \iint_{\Omega} \mathbf{\Pi}^T : \nabla\underline{\psi}\ \mathrm{d}X_1\mathrm{d}X_2. \tag{4.13}$$

We use this in the weak form of the equations of motion.

Let $\underline{V} = \dot{\underline{U}}$ denote the velocity vector. We describe the equations of motion in the general 3D case in partial differential equation form as the system

$$\rho\dot{\underline{V}} = \text{Div}\,\mathbf{\Pi}_{3D}, \quad \text{where Div}\,\mathbf{\Pi}_{3D} = \begin{pmatrix} \frac{\partial\Pi_{11}}{\partial X_1} + \frac{\partial\Pi_{21}}{\partial X_2} + \frac{\partial\Pi_{31}}{\partial X_3} \\ \frac{\partial\Pi_{12}}{\partial X_1} + \frac{\partial\Pi_{22}}{\partial X_2} + \frac{\partial\Pi_{32}}{\partial X_3} \\ \frac{\partial\Pi_{13}}{\partial X_1} + \frac{\partial\Pi_{23}}{\partial X_2} + \frac{\partial\Pi_{33}}{\partial X_3} \end{pmatrix}, \tag{4.14}$$

$$\underline{V} = \dot{\underline{U}}\,. \tag{4.15}$$

To complete this form of the description we need initial conditions $\underline{U}(\underline{X}, 0) = \underline{U}^0$, $\underline{V}(\underline{X}, 0) = \underline{V}^0$, boundary conditions (i.e. on $\partial\Omega$) and a constitutive model relating the stress $\mathbf{\Pi}_{3D}$ to $\mathbf{F}_{3D}$. For the computational model and the error representation formula we need a weak form which can be obtained as follows. We take the dot product of (4.14) with $\underline{\psi}$ and integrate over the space time domain

$$Q = \Omega \times (0, T) \tag{4.16}$$

and we similarly take the dot product of (4.15) with $\underline{\theta}$ and integrate over Q. From the terms involving $\underline{\psi}$ we can re-express things using the divergence theorem which brings in the pressure loading term $P = P(t)$ and we can make use of (4.13). Assuming that $\underline{\psi} = \underline{0}$ on $\partial\Omega$ we have

$$\begin{aligned} \int_{\Omega_{3D}} \text{Div}\,\mathbf{\Pi}_{3D} \cdot \underline{\psi}\,\mathrm{d}\underline{X} &= -\int_{\Omega_{3D}} \mathbf{\Pi}_{3D}^T : \nabla_{3D}\underline{\psi}\,\mathrm{d}\underline{X} + P\iint_{\Omega} (\underline{f}_1 \times \underline{f}_2) \cdot \underline{\psi}\,\mathrm{d}X_1\mathrm{d}X_2, \\ &\approx -h_0 \iint_{\Omega} \mathbf{\Pi}^T : \nabla\underline{\psi}\,\mathrm{d}X_1\mathrm{d}X_2 + P\iint_{\Omega} (\underline{f}_1 \times \underline{f}_2) \cdot \underline{\psi}\,\mathrm{d}X_1\mathrm{d}X_2, \end{aligned}$$

where $\underline{f}_1$ and $\underline{f}_2$ are the first two columns of $\mathbf{F}$ given in (4.7). We combine the terms involving $\underline{\psi}$ and the terms involving $\underline{\theta}$ into a single expression in which the initial conditions are only imposed weakly. In the following we collect together the unknowns $\underline{U}$, $\underline{V}$ and the test vectors $\underline{\psi}$, $\underline{\theta}$ as

$$\begin{pmatrix} \underline{U} \\ \underline{V} \end{pmatrix} \quad \text{and} \quad \begin{pmatrix} \underline{\psi} \\ \underline{\theta} \end{pmatrix}. \tag{4.17}$$

In the expressions that follow we use the usual inner product notation $(.,.)_G$ to mean

$$(f,g)_G := \int_G fg \, \mathrm{d}G, \tag{4.18}$$

where in our case $G = \Omega$ or $G = Q$. Our weak forms are as follows.

In the quasi-static case we ignore the $\rho\dot{\underline{V}}$ term and we have

$$a(\underline{U};\underline{\psi})_\Omega = 0, \quad \text{for all appropriate } \underline{\psi}, \quad \text{for } 0 < t \leq T \tag{4.19}$$

where

$$a(\underline{U};\underline{\psi})_\Omega := a_1(\underline{U};\underline{\psi})_\Omega - P(t)a_2(\underline{U};\underline{\psi})_\Omega \tag{4.20}$$

and where

$$a_1(\underline{U};\underline{\psi}) = h_0 \int_\Omega \mathbf{\Pi}^T : \nabla\underline{\psi} \, \mathrm{d}\underline{X}\mathrm{d}t, \tag{4.21}$$

$$a_2(\underline{U};\underline{\psi}) = \int_\Omega (\underline{f}_1 \times \underline{f}_2) \cdot \underline{\psi} \, \mathrm{d}\underline{X}\mathrm{d}t. \tag{4.22}$$

In the full dynamic case we include the $\rho\dot{\underline{V}}$ term and we have

$$A(\begin{pmatrix}\underline{U}\\ \underline{V}\end{pmatrix};\begin{pmatrix}\underline{\psi}\\ \underline{\theta}\end{pmatrix}) = F(\begin{pmatrix}\underline{\psi}\\ \underline{\theta}\end{pmatrix}), \quad \text{for all appropriate } \underline{\psi} \text{ and } \underline{\theta}, \tag{4.23}$$

where

$$\begin{aligned} A(\begin{pmatrix}\underline{U}\\ \underline{V}\end{pmatrix};\begin{pmatrix}\underline{\psi}\\ \underline{\theta}\end{pmatrix}) &:= a(\underline{U};\underline{\psi})_Q + \rho h_0(\dot{\underline{V}},\underline{\psi})_Q \\ &\quad + \rho h_0 \left((\dot{\underline{U}} - \underline{V},\underline{\theta})_Q + (\underline{U}(.,0),\underline{\theta})_\Omega + (\underline{V}(.,0),\underline{\psi})_\Omega \right), \end{aligned} \tag{4.24}$$

$$F(\begin{pmatrix}\underline{\psi}\\ \underline{\theta}\end{pmatrix}) := \rho h_0(\underline{U}^0,\underline{\theta})_\Omega + \rho h_0(\underline{V}^0,\underline{\psi})_\Omega \tag{4.25}$$

where $a(.,.)_Q$ involves the same expression as in the quasi-static case except that now integration is over Q. Specifically we have

$$a(\underline{U};\underline{\psi})_Q = a_1(\underline{U};\underline{\psi})_Q - a_2(\underline{U};\underline{\psi})_Q \tag{4.26}$$

with

$$a_1(\underline{U};\underline{\psi})_Q = \int_0^T \int_\Omega \tilde{a}(\underline{U};\underline{\psi}) \, \mathrm{d}\underline{X}\mathrm{d}t \quad \text{and} \quad a_2(\underline{U};\underline{\psi})_Q = \int_0^T \int_\Omega P(t)\tilde{a}_2(\underline{U};\underline{\psi}) \, \mathrm{d}\underline{X}\mathrm{d}t \tag{4.27}$$

with the integrand expressions being

$$\tilde{a}_1(\underline{U};\underline{\psi}) = h_0\mathbf{\Pi}^T : \nabla\underline{\psi} \quad \text{and} \quad \tilde{a}_2(\underline{U};\underline{\psi}) = (\underline{f}_1 \times \underline{f}_2) \cdot \underline{\psi}. \tag{4.28}$$

The dependence of $\mathbf{\Pi}$ on $\underline{U}$ for a hyperelastic material depends on the form of the strain energy function W and can be expressed in the form

$$\mathbf{\Pi}^T = \frac{\partial W}{\partial \mathbf{F}} \tag{4.29}$$

with an appropriate interpretation of the meaning of the partial derivatives. In the case of an axi-symmetric deformation and an isotropic material we can give more explicit representations of the $\tilde{a}(\underline{U};\underline{\psi})$ term. In this case we have $W = W(\lambda_1, \lambda_2)$ where

$$\lambda_1^2 = (1+U_1')^2 + U_3'^2 \quad \text{and} \quad \lambda_2 = 1 + \frac{U_1}{r} \tag{4.30}$$

are the principal stretch ratios. Then it can be shown that the principal stresses are given by

$$\sigma_1 = \lambda_1 \frac{\partial W}{\partial \lambda_1} \quad \text{and} \quad \sigma_2 = \lambda_2 \frac{\partial W}{\partial \lambda_2}. \tag{4.31}$$

To simplify the notation a little we let

$$W_1 := \frac{\partial W}{\partial \lambda_1}, \quad W_2 := \frac{\partial W}{\partial \lambda_2}, \quad W_{11} := \frac{\partial^2 W}{\partial \lambda_1^2}, \quad W_{22} := \frac{\partial^2 W}{\partial \lambda_2^2}, \quad W_{12} = W_{21} := \frac{\partial^2 W}{\partial \lambda_1 \partial \lambda_2}. \tag{4.32}$$

Using this notation it follows that the nominal stress components are given by

$$\Pi_{11} = \frac{\sigma_1}{\lambda_1^2}(1+U_1') = \frac{W_1}{\lambda_1}(1+U_1'), \quad \Pi_{13} = \frac{\sigma_1}{\lambda_1^2}U_3' = \frac{W_1}{\lambda_1}U_3', \quad \Pi_{22} = \frac{\sigma_2}{\lambda_2} = W_2. \tag{4.33}$$

Then by noting that $\mathrm{d}\underline{X} = r\mathrm{d}r$ and letting $\underline{U} = (U_1, U_3)^T$ and $\underline{V} = (V_1, V_3)^T$ we have

$$\tilde{a}_1(\underline{U};\underline{\psi}) = h_0 \left(\frac{W_1}{\lambda_1}((1+U_1')\psi_1' + U_3'\psi_3') + W_2 \frac{\psi_1}{r} \right), \tag{4.34}$$

$$\tilde{a}_2(\underline{U};\psi) = \left(1 + \frac{U_1}{r}\right)(-U_3'\psi_1 + (1+U_1')\psi_3). \tag{4.35}$$

To complete the description and to add some rigor we need to indicate the function spaces for $\underline{U}, \underline{V}$ and $\underline{\psi}, \underline{\tau}$ given in (4.17) and (4.23) and similarly we need to give the spaces for the test vectors $\underline{\psi}$ and $\underline{\theta}$. Note that we have first spatial derivatives of the displacement $\underline{U}$ but not for the velocity $\underline{V}$ and we have first time derivatives of both $\underline{U}$ and $\underline{V}$. For the test vectors we have first spatial derivatives of $\underline{\psi}$ but there are no spatial derivatives of $\underline{\theta}$ and there are no time derivatives on either function. Hence, as in [1, p.264], the unknowns and test vectors are such that

$$\underline{U} \in H^1((0,T), H^1(\Omega)), \qquad \underline{V} \in H^1((0,T), L_2(\Omega)), \tag{4.36}$$

$$\underline{\psi} \in L_2((0,T), H^1(\Omega)), \qquad \underline{\theta} \in L_2((0,T), L_2(\Omega)). \tag{4.37}$$

The functions $\underline{\psi}$ vanish on the part of $\partial\Omega$ where Dirichlet boundary conditions are imposed.

As a final comment about imposing the initial conditions weakly we note that the displacement initial conditions that we consider are such that $\underline{U}^0 = \underline{0}$ or $\underline{U}^0$ corresponds to a uniform pre-stretch are in fact satisfied exactly.

4.2 $\tilde{a}_1(.;.)$ and $\tilde{a}_2(.;.)$ as derivatives of functionals

The term $\tilde{a}_1(\underline{U};\underline{\psi})$ and the integral over $(0,1)$ of $\tilde{a}_2(\underline{U};\underline{\psi})$ defined in (4.28) are in fact Gateaux derivatives of appropriate functionals, i.e. they are of the form

$$r\tilde{a}_1(\underline{U};\underline{\psi}) = g_1'(\underline{U};\underline{\psi}) \quad \text{and} \quad \int_0^1 \tilde{a}_2(\underline{U};\underline{\psi})\, r\mathrm{d}r = \int_0^1 g_2'(\underline{U};\underline{\psi}) r\, \mathrm{d}r \tag{4.38}$$

for certain functionals g_1 and g_2. As a consequence, when we consider the dual problem and when methods for solving the dynamic problem are considered we have to consider terms of the form

$$r\tilde{a}_1'(\underline{U};\underline{\alpha},\underline{\psi}) = g_1''(\underline{U};\underline{\alpha},\underline{\psi}), \quad \text{and} \quad \int_0^1 \tilde{a}_2'(\underline{U};\underline{\alpha},\underline{\psi})\, r\mathrm{d}r \int_0^1 g_2''(\underline{U};\underline{\alpha},\underline{\psi})\, r\mathrm{d}r \tag{4.39}$$

which are thus symmetric in $\underline{\alpha}$ and $\underline{\psi}$ and as a consequence we can construct our algorithms in such a way that each linear system that we have to solve has a symmetric matrix.

The functionals g_1 and g_2 for the axisymmetric case are as follows.

$$g_1(\underline{U}) := rh_0 W \quad \text{and} \quad g_2(\underline{U}) := \frac{1}{3}(r+U_1)(-(r+U_1)U_3' + (1+U_1')U_3). \tag{4.40}$$

We can verify directly that the first Gateaux derivatives of these do indeed give the expressions for $\tilde{a}_1(.;.)$ and $\tilde{a}_2(.;.)$ as follows.

We first consider the g_1 term and we use the notation here that $\underline{U}(s) = \underline{U} + s\underline{\psi}$ where $\underline{\psi}$ is the function which we differentiate in the direction of. We similarly let $\lambda_1(s)$ and $\lambda_2(s)$ be the stretch ratios that we get with $\underline{U}(s)$. We need to differentiate with respect to s and evaluate the derivatives at $s = 0$. This gives

$$\lambda_1'(\underline{U};\underline{\psi}) = \left.\frac{\mathrm{d}\lambda_1}{\mathrm{d}s}\right|_{s=0} = \frac{(1+U_1')\psi_1' + U_3'\psi_3'}{\lambda_1} \quad \text{and} \quad \lambda_2'(\underline{U};\underline{\psi}) = \left.\frac{\mathrm{d}\lambda_2}{\mathrm{d}s}\right|_{s=0} = \frac{\psi_1}{r}. \tag{4.41}$$

Then as $W = W(\lambda_1, \lambda_2)$ the chain rule gives

$$g_1'(\underline{U};\underline{\psi}) = rh_0 \left(W_1\, \lambda_1'(\underline{U};\underline{\psi}) + W_2\, \lambda_2'(\underline{U};\underline{\psi})\right) \tag{4.42}$$

and we get the term $r\tilde{a}_2(\underline{U};\underline{\psi})$, see (4.34).

Next we consider the g_2 term which is connected with the pressure loading and again use the notation that $\underline{U}(s) = \underline{U} + s\underline{\psi}$ where $\underline{\psi}$ is the function which we differentiate in the direction of so that

$$3g_2(\underline{U}(s)) = (r+U_1+s\psi_1)(-(r+U_1+s\psi_1)(U_3'+s\psi_3') + (1+U_1+s\psi_1')(U_3+s\psi_3)). \tag{4.43}$$

Differentiating with respect to s and evaluating at $s = 0$ gives

$$3g_2'(\underline{U};\underline{\psi}) = \psi_1(-(r+U_1)U_3' + (1+U_1')U_3) + (r+U_1)(-\psi_1 U_3' - (r+U_1)\psi_3' + \psi_1' U_3 + (1+U_1')\psi_3). \tag{4.44}$$

It is the integral of this over the space domain that we need to consider and we can re-express things using integration by parts on the ψ_1' and ψ_3' terms. Observe that since ψ_1 and ψ_3 are zero at $r = 1$ we have

$$-\int_0^1 (r+U_1)^2\psi_3'\,\mathrm{d}r = 2\int_0^1 (r+U_1)(1+U_1')\psi_3\,\mathrm{d}r \tag{4.45}$$

and

$$\int_0^1 (r+U_1)U_3\psi_1'\,\mathrm{d}r = -\int_0^1 ((r+U_1)U_3' + (1+U_1')U_3)\psi_1\,\mathrm{d}r. \tag{4.46}$$

Hence

$$3\int_0^1 g_2'(\underline{U};\underline{\psi})\,\mathrm{d}r = 3\int_0^1 (r+U_1)(-U_3'\psi_1 + (1+U_1')\psi_3)\,\mathrm{d}r = 3\int_0^1 \tilde{a}_2(\underline{U};\underline{\psi})\, r\mathrm{d}r. \tag{4.47}$$

4.3 The Gateaux derivative $A'(.;.,.)$ for the dual problem obtained from the dynamic problem

For the dual problem in this context we need the Gateaux derivative of the following in a direction such as $\begin{pmatrix}\underline{\alpha}\\ \underline{\beta}\end{pmatrix}$, where $\underline{\alpha} = \begin{pmatrix}\alpha_1\\ \alpha_3\end{pmatrix}$, $\underline{\beta} = \begin{pmatrix}\beta_1\\ \beta_3\end{pmatrix}$. With this notation we have, in vector notation,

$$\begin{aligned} A(\begin{pmatrix}\underline{U}\\ \underline{V}\end{pmatrix};\begin{pmatrix}\underline{\psi}\\ \underline{\theta}\end{pmatrix}) \;&:=\; a(\underline{U};\underline{\psi})_Q + \rho h_0(\dot{\underline{V}},\underline{\psi})_Q \\ &\quad +\rho h_0\left((\dot{\underline{U}}-\underline{V},\underline{\theta})_Q + (\underline{U}(.,0),\underline{\theta})_\Omega + (\underline{V}(.,0),\underline{\psi})_\Omega\right), \end{aligned} \tag{4.48}$$

which gives

$$\begin{aligned} A(\begin{pmatrix}\underline{U}\\ \underline{V}\end{pmatrix} + s\begin{pmatrix}\underline{\alpha}\\ \underline{\beta}\end{pmatrix};\begin{pmatrix}\underline{\psi}\\ \underline{\theta}\end{pmatrix}) \;&:=\; a(\underline{U}+s\underline{\alpha};\underline{\psi})_Q + \rho h_0(\dot{\underline{V}}+s\dot{\underline{\beta}},\underline{\psi})_Q \\ &\quad +\rho h_0\left((\dot{\underline{U}}-\underline{V}+s(\dot{\underline{\alpha}}-\underline{\beta}),\underline{\theta})_Q + (\underline{U}(.,0)+s\underline{\alpha}(.,0),\underline{\theta})_\Omega\right. \\ &\quad \left.+(\underline{V}(.,0)+s\underline{\beta}(.,0),\underline{\psi})_\Omega\right). \end{aligned} \tag{4.49}$$

Thus

$$\begin{aligned} A'(\begin{pmatrix}\underline{U}\\ \underline{V}\end{pmatrix};\begin{pmatrix}\underline{\alpha}\\ \underline{\beta}\end{pmatrix},\begin{pmatrix}\underline{\psi}\\ \underline{\theta}\end{pmatrix}) \;&=\; A'(\underline{U};\underline{\alpha},\underline{\psi})_Q + \rho h_0(\dot{\underline{\beta}},\underline{\psi})_Q \\ &\quad +\rho h_0\left((\dot{\underline{\alpha}}-\underline{\beta},\underline{\theta})_Q + (\underline{\alpha}(.,0),\underline{\theta})_\Omega + (\underline{\beta}(.,0),\underline{\psi})_\Omega\right) \qquad (4.50) \\ &=\; A'(\underline{U};\underline{\alpha},\underline{\psi})_Q - \rho h_0(\underline{\beta},\dot{\underline{\psi}})_Q \\ &\quad +\rho h_0\left(-(\underline{\alpha},\dot{\underline{\theta}})_Q - (\underline{\beta},\underline{\theta})_Q + (\underline{\alpha}(.,T),\underline{\theta})_\Omega + (\underline{\beta}(.,T),\underline{\psi})_\Omega\right) \qquad (4.51) \end{aligned}$$

In the first version in (4.50) there are time derivatives on $\begin{pmatrix}\underline{\alpha}\\ \underline{\beta}\end{pmatrix}$ whilst in the second version in (4.50), which was obtained by integration by parts in time, there are no time derivatives on $\begin{pmatrix}\underline{\alpha}\\ \underline{\beta}\end{pmatrix}$. This is the form of $A'(.;.,.)$ that we need in the dual problem for finding $\underline{\psi}$ and $\underline{\theta}$ such that

$$A'(\begin{pmatrix}\underline{U}\\ \underline{V}\end{pmatrix};\begin{pmatrix}\underline{\alpha}\\ \underline{\beta}\end{pmatrix},\begin{pmatrix}\underline{\psi}\\ \underline{\theta}\end{pmatrix}) = J'(\begin{pmatrix}\underline{U}\\ \underline{V}\end{pmatrix};\begin{pmatrix}\underline{\alpha}\\ \underline{\beta}\end{pmatrix}) \quad \text{for all suitable } \begin{pmatrix}\underline{\alpha}\\ \underline{\beta}\end{pmatrix}. \tag{4.52}$$

The "for all suitable $\underline{\alpha}$ and $\underline{\beta}$" condition in particular requires that the components of $\underline{\alpha}(r,t)$ and $\underline{\beta}(r,t)$ vanish wherever the components of $\underline{U}(r,t)$ or $\underline{V}(r,t)$ have a Dirichlet boundary condition and hence in this application we have $\alpha_1(0,t) = \beta_1(0,t) = 0$ (corresponding to the axisymmetric condition) and $\underline{\alpha}(1,t) = \underline{\beta}(1,t) = 0$ (corresponding to the clamped edge boundary condition).

A general form of a suitable $J(.)$ is given by

$$J(\begin{pmatrix}\underline{U}\\ \underline{V}\end{pmatrix}) \;=\; \int_0^T\int_0^1 r\{\text{expression in } \underline{U},\underline{V},\underline{U}',\underline{V}'\}\,\mathrm{d}r\mathrm{d}t \tag{4.53}$$

$$+\int_0^1 r\{\text{expression in } \underline{U}(.,T),\underline{V}(.,T),\underline{U}'(.,T),\underline{V}'(.,T)\}\,\mathrm{d}r\mathrm{d}t. \tag{4.54}$$

There should be no time derivatives in the integrand expressions. The Gateaux derivative of such a $J(.)$ is of the form

$$J'(\begin{pmatrix}\underline{U}\\ \underline{V}\end{pmatrix};\begin{pmatrix}\underline{\alpha}\\ \underline{\beta}\end{pmatrix}) = \int_0^T\int_0^1 (\underline{\alpha}\cdot\underline{J}_\alpha + \underline{\beta}\cdot\underline{J}_\beta + \underline{\alpha}'\cdot\underline{J}_{\alpha'} + \underline{\beta}'\cdot\underline{J}_{\beta'})\, r\mathrm{d}r\mathrm{d}t \quad (4.55)$$

$$+\int_0^1 (\underline{\alpha}(r,T)\cdot\underline{J}_\alpha(r,T) + \underline{\beta}(r,T)\cdot\underline{J}_\beta(r,T) \quad (4.56)$$

$$\underline{\alpha}'(r,T)\cdot\underline{J}_{\alpha'}(r,T) + \underline{\beta}'(r,T)\cdot\underline{J}_{\beta'}(r,T))\, r\mathrm{d}r. \quad (4.57)$$

By considering the $\underline{\alpha}(.,T)$ and $\underline{\beta}(.,T)$ terms we get conditions on $\underline{\psi}$ and $\underline{\theta}$ at time $t=T$ which are

$$\rho h_0(\underline{\alpha}(.,T),\underline{\theta}(.,T))_\Omega = \int_0^1 (\underline{\alpha}(r,T)\cdot\underline{J}_\alpha(r,T) + \underline{\alpha}'(r,T)\cdot\underline{J}_{\alpha'}(r,T))\, r\mathrm{d}r, \quad (4.58)$$

$$\rho h_0(\underline{\beta}(.,T),\underline{\psi}(.,T))_\Omega, = \int_0^1 (\underline{\beta}(r,T)\cdot\underline{J}_\beta(r,T) + \underline{\beta}'(r,T)\cdot\underline{J}_{\beta'}(r,T))\, r\mathrm{d}r \quad (4.59)$$

which must hold for all suitable $\underline{\alpha}(r,T)$ and $\underline{\beta}(r,T)$. By considering the $\underline{\beta}(r,t)$ terms for $0\le t<T$ we get

$$-\rho h_0(\dot{\underline{\psi}}+\underline{\theta},\underline{\beta})_Q = \int_0^T\int_0^1 \underline{\beta}\cdot\underline{J}_\beta + \underline{\beta}'\cdot\underline{J}_{\beta'}\; r\mathrm{d}r\mathrm{d}t. \quad (4.60)$$

Similarly, considering the $\underline{\alpha}(r,t)$ terms for $0\le t<T$ we get

$$a'(\underline{U};\underline{\alpha},\underline{\psi})_Q - \rho h_0(\underline{\alpha},\dot{\underline{\theta}})_Q = \int_0^T\int_0^1 \underline{\alpha}\cdot\underline{J}_\alpha + \underline{\alpha}'\cdot\underline{J}_{\alpha'}\; r\mathrm{d}r\mathrm{d}t. \quad (4.61)$$

The equations (4.58), (4.59), (4.60) and (4.61) give a linear problem for $\underline{\psi}$ and $\underline{\theta}$ which has a structure which is similar to the problem of determining the displacement $\underline{U}$ and the velocity $\underline{V}$ although with some key differences. For the dual problem we have final time conditions (i.e. at $t=T$) instead of initial conditions. Equation (4.60) is similar to the condition $\dot{\underline{U}}=\underline{V}$ which is imposed weakly. Equation (4.61) involves the term $a'(.;.,.)$ which is encountered in numerical schemes for approximately solving for $\underline{U}$ and $\underline{V}$ by using a Newton iteration. Recall from the discussion in section 4.2 that $a'(\underline{U};\underline{\alpha},\underline{\psi})_Q$ is unchanged if we swap $\underline{\alpha}$ and $\underline{\psi}$.

4.4 Expressions for $a_1'(\underline{U};\underline{\alpha},\underline{\psi})_Q$ and $a_2'(\underline{U};\underline{\alpha},\underline{\psi})_Q$

We now complete the details of the dual problem by giving expressions for the $a_1'(.;.,.)_Q$ and $a_2'(.;.,.)_Q$ terms needed in (4.61).

Recall that we have already shown that

$$r\tilde{a}(\underline{U};\underline{\psi}) = g_1'(\underline{U};\underline{\psi}) = rh_0\left(W_1\,\lambda_1'(\underline{U};\underline{\psi}) + W_2\,\lambda_2'(\underline{U};\underline{\psi})\right). \quad (4.62)$$

Taking now the Gateaux derivative in the direction of $\underline{\alpha}$ we have

$$\begin{aligned} r\tilde{a}_1'(\underline{U};\underline{\alpha},\underline{\psi}) &= rh_0\left((W_{11}\lambda_1'(\underline{U};\underline{\alpha}) + W_{12}\lambda_2'(\underline{U};\underline{\alpha}))\lambda_1'(\underline{U};\underline{\psi}) + W_1\lambda_1''(\underline{U};\underline{\alpha},\underline{\psi})\right.\\ &\quad \left. + (W_{12}\lambda_1'(\underline{U};\underline{\alpha}) + W_{22}\lambda_2'(\underline{U};\underline{\alpha}))\lambda_2'(\underline{U};\underline{\psi}) + W_2\lambda_2''(\underline{U};\underline{\alpha},\underline{\psi})\right)\\ &= rh_0\left(W_{11}\lambda_1'(\underline{U};\underline{\alpha})\lambda_1'(\underline{U};\underline{\psi}) + W_{22}\lambda_2'(\underline{U};\underline{\alpha})\lambda_2'(\underline{U};\underline{\psi})\right.\\ &\quad +W_{12}(\lambda_1'(\underline{U};\underline{\alpha})\lambda_2'(\underline{U};\underline{\psi}) + \lambda_1'(\underline{U};\underline{\psi})\lambda_2'(\underline{U};\underline{\alpha}))\\ &\quad \left.+(W_1\lambda_1''(\underline{U};\underline{\alpha},\underline{\psi}) + W_2\lambda_2''(\underline{U};\underline{\alpha},\underline{\psi}))\right). \end{aligned} \quad (4.63)$$

The first Gateaux derivatives of the stretch ratios are given in (4.41), i.e.

$$\lambda_1'(\underline{U};\underline{\psi}) = \frac{(1+U_1')\psi_1' + U_3'\psi_3'}{\lambda_1}, \qquad \lambda_1'(\underline{U};\underline{\alpha}) = \frac{(1+U_1')\alpha_1' + U_3'\alpha_3'}{\lambda_1}, \tag{4.64}$$

$$\lambda_2'(\underline{U};\underline{\psi}) = \frac{\psi_1}{r}, \qquad \lambda_2'(\underline{U};\underline{\alpha}) = \frac{\alpha_1}{r}. \tag{4.65}$$

For the second Gateaux derivatives of the stretch ratios we immediately have $\lambda_2''(\underline{U};\underline{\alpha},\underline{\psi}) = 0$. For the second derivative of λ_1 we have

$$\lambda_1\lambda_1''(\underline{U};\underline{\alpha},\underline{\psi}) + \lambda_1'(\underline{U};\underline{\alpha})\lambda_1'(\underline{U};\underline{\psi}) = \alpha_1'\psi_1' + \alpha_3'\psi_3' \tag{4.66}$$

and hence

$$\lambda_1''(\underline{U};\underline{\alpha},\underline{\psi}) = \frac{\alpha_1'\psi_1' + \alpha_3'\psi_3' - \lambda_1'(\underline{U};\underline{\alpha})\lambda_1'(\underline{U};\underline{\psi})}{\lambda_1}. \tag{4.67}$$

Now, from (4.35) we have

$$a_2(\underline{U};\underline{\psi})_Q = \int_0^T \int_0^1 P(t)\,\tilde{a}_2(\underline{U};\underline{\psi})\,r\mathrm{d}r\mathrm{d}t, \tag{4.68}$$

where

$$r\tilde{a}_2(\underline{U};\underline{\psi}) = (r+U_1)(-U_3'\psi_1 + (1+U_1')\psi_3) \tag{4.69}$$

and from this it follows that

$$r\tilde{a}_2'(\underline{U};\underline{\alpha},\underline{\psi}) = (r+U_1)(-\alpha_3'\psi_1 + \alpha_1'\psi_3) + \alpha_1(-U_3'\psi_1 + (1+U_1')\psi_3). \tag{4.70}$$

It is the integral of this that we need and by using integration by parts on the last term and noting that α_1 and ψ_3 vanish at $r=1$ we have

$$\int_0^1 \alpha_1\psi_3(1+U_1')\,\mathrm{d}r = -\int_0^1 (\alpha_1\psi_3' + \alpha_1'\psi_3)(r+U_1)\,\mathrm{d}r. \tag{4.71}$$

Hence

$$\int_0^1 r\tilde{a}_2'(\underline{U};\underline{\alpha},\underline{\psi})\,\mathrm{d}r = -\int_0^1 (U_3'\alpha_1\psi_1 + (r+U_1)(\alpha_3'\psi_1 + \psi_3'\alpha_1))\,\mathrm{d}r. \tag{4.72}$$

Again we have a quantity which is symmetric in $\underline{\alpha}$ and $\underline{\psi}$ as explained previously.

4.5 A summary of the dual equation in the dynamic case

To summarize, the dual problem is as given in (4.52), i.e. it is the linear problem of finding $\begin{pmatrix}\underline{\psi}\\ \underline{\theta}\end{pmatrix}$ such that

$$A'(\begin{pmatrix}\underline{U}\\ \underline{V}\end{pmatrix};\begin{pmatrix}\underline{\alpha}\\ \underline{\beta}\end{pmatrix},\begin{pmatrix}\underline{\psi}\\ \underline{\theta}\end{pmatrix}) = J'(\begin{pmatrix}\underline{U}\\ \underline{V}\end{pmatrix};\begin{pmatrix}\underline{\alpha}\\ \underline{\beta}\end{pmatrix}) \quad \text{for all suitable } \begin{pmatrix}\underline{\alpha}\\ \underline{\beta}\end{pmatrix} \tag{4.73}$$

where $A'(\begin{pmatrix}\underline{U}\\ \underline{V}\end{pmatrix};.,.)$ can be written as

$$\begin{aligned} A'(\begin{pmatrix}\underline{U}\\ \underline{V}\end{pmatrix};\begin{pmatrix}\underline{\alpha}\\ \underline{\beta}\end{pmatrix},\begin{pmatrix}\underline{\psi}\\ \underline{\theta}\end{pmatrix}) \;=\; & a'(\underline{U};\underline{\alpha},\underline{\psi})_Q - \rho h_0(\underline{\alpha},\dot{\underline{\theta}})_Q - \rho h_0(\underline{\beta},\dot{\underline{\psi}}+\underline{\theta})_Q \\ & +\rho h_0(\underline{\alpha}(.,T),\underline{\theta})_\Omega + \rho h_0(\underline{\beta}(.,T),\underline{\psi})_\Omega \end{aligned} \tag{4.74}$$

and $J'(.;.)$ is of the form

$$J'(\begin{pmatrix}\underline{U}\\ \underline{V}\end{pmatrix};\begin{pmatrix}\underline{\alpha}\\ \underline{\beta}\end{pmatrix}) = \int_0^T\int_0^1 (\underline{\alpha}\cdot\underline{J}_\alpha + \underline{\beta}\cdot\underline{J}_\beta + \underline{\alpha}'\cdot\underline{J}_{\alpha'} + \underline{\beta}'\cdot\underline{J}_{\beta'})\, r\mathrm{d}r\mathrm{d}t$$
$$+\int_0^1 (\underline{\alpha}(r,T)\cdot\underline{J}_\alpha(r,T) + \underline{\beta}(r,T)\cdot\underline{J}_\beta(r,T)$$
$$\underline{\alpha}'(r,T)\cdot\underline{J}_{\alpha'}(r,T) + \underline{\beta}'(r,T)\cdot\underline{J}_{\beta'}(r,T))\, r\mathrm{d}r. \tag{4.75}$$

Note that $A'(.;.,.)$ does not actually depend on the velocity $\underline{V}$. By using (4.63) and the subsequent expressions we have

$$a'(\underline{U};\underline{\alpha},\underline{\psi})_Q = \int_0^T\int_0^1 r\tilde{a}_3(\underline{U};\underline{\alpha},\underline{\psi})\,\mathrm{d}r\mathrm{d}t \tag{4.76}$$

with

$$\tilde{a}_3(\underline{U};\underline{\alpha},\underline{\psi}) = (\alpha_1,\alpha_1',\alpha_3')G\begin{pmatrix}\psi_1\\ \psi_1'\\ \psi_3'\end{pmatrix} \tag{4.77}$$

and with the symmetric 3×3 matrix G given by

$$G = h_0G_1 - P(t)G_2 \tag{4.78}$$

where

$$G_1 = \begin{pmatrix} \frac{W_{22}}{r^2} & \frac{W_{12}}{r}\frac{(1+U_1')}{\lambda_1} & \frac{W_{12}}{r}\frac{U_3'}{\lambda_1}\\ \frac{W_{12}}{r}\frac{(1+U_1')}{\lambda_1} & W_{11}\frac{(1+U_1')^2}{\lambda_1^2} + W_1\frac{U_3'^2}{\lambda_1^3} & \frac{(1+U_1')U_3'}{\lambda_1^2}\left(W_{11}-\frac{W_1}{\lambda_1}\right)\\ \frac{W_{12}}{r}\frac{U_3'}{\lambda_1} & \frac{(1+U_1')U_3'}{\lambda_1^2}\left(W_{11}-\frac{W_1}{\lambda_1}\right) & W_{11}\frac{U_3'^2}{\lambda_1^2} + W_1\frac{(1+U_1')^2}{\lambda_1^3}\end{pmatrix} \tag{4.79}$$

and

$$G_2 = \begin{pmatrix} -\frac{U_3'}{r} & 0 & -\left(1+\frac{U_1}{r}\right)\\ 0 & 0 & 0\\ -\left(1+\frac{U_1}{r}\right) & 0 & 0\end{pmatrix}. \tag{4.80}$$

5 Implementation: Computational schemes

In this section we describe the computational schemes used for the quasi-static problem, the dynamic problem and for the dual problem derived from the dynamic problem. As already indicated, the quasi-static and dynamic problems are nonlinear and require an iteration and a Newton iteration is used here. In all cases we have a spatial discretization and in the last two cases we have a space-time discretization. Time levels are actually also needed when we consider quasi-static problems in possibly two different ways. They provide the means for generating sufficiently good starting points for the Newton iterations, i.e. when we seek the solution at the loading level $P(t_j)$ at time t_j we can use the solution at the previous time t_{j-1} to start the Newton iteration with guaranteed convergence if $P(t_j) - P(t_{j-1})$ is sufficiently small and we are not too close to critical points. A sufficient

number of time levels is also needed in cases when the QoI involves the velocity and the purpose of the computation is to predict this QoI using just the quasi-static solution.

As we have explained in the previous sections, the procedure of constructing an approximate dual problem and having a solution z_h to such a problem enables us to be able to estimate the error in an approximation $J(u_h)$ to a QoI $J(U)$ in a relation of the form

$$J(U) - J(u_h) \approx F(z_h) - A(u_h; z_h). \tag{5.1}$$

In situations when we only have discretization error we can make further use of z_h to determine how we should adaptively refine the mesh in order to create an approximation $J(u_h)$ for which $|F(z) - A(u_h; z_h)|$ is at or below a desired tolerance. We describe how this is done in the case of the quasi-static inflation problem in subsection 5.5.

5.1 Notation and things common to all the problems

Much of the notation used in the description is common to all the problems and thus we give first the notation for the space and time discretization and we give the piecewise polynomial form for the vectors, i.e. $\underline{u}$, $\underline{v}$, $\underline{\psi}$ and $\underline{\theta}$, in the computational schemes after a discussion about the spaces that the exact solutions to each problem are in.

5.1.1 The mesh points

For the discretization we assume that there are $N + 1$ time levels

$$0 = t_0 < t_1 < t_2 < \cdots < t_N = T \tag{5.2}$$

and a fixed mesh of $\tilde{M}$ space elements (r_{i-1}, r_i) where

$$0 = r_0 < r_1 < r_2 < \cdots < r_{\tilde{M}} = 1. \tag{5.3}$$

The meshes used need not be the same for each problem.

5.1.2 Remarks about the function spaces for $\underline{U}$, $\underline{V}$, $\underline{\psi}$ and $\underline{\theta}$

In section 4 we derived the expressions for $a(.;.)$, $A(.;.)$ and $A'(.;.,.)$ without too much comment as to the spaces in which the various terms should be in. In fact, for the nonlinear problems you cannot specify precisely the function space for the displacement $\underline{U}$ until you have specified the form of the strain energy function $W = W(\lambda_1, \lambda_2)$ in order to know which powers of

$$\lambda_1 = ((1 + U_1')^2 + U_3'^2)^{1/2} \quad \text{and} \quad \lambda_2 = 1 + \frac{U_1}{r} \tag{5.4}$$

appear. Also, even when you are in a position to specify a function space, so that $a(\underline{U};.)$ and $A(\underline{U};.)$ are properly defined for all $\underline{U}$ in the space, there is still likely to be a far bit of additional analysis needed to determine if such a problem has a unique solution from the space. A rigorous mathematical analysis of which space U_1 and U_3 are in, to the extent of determining the values of $q \geq 1$ such that $U_i' \in L_q(\Omega)$, does not actually affect how we choose the finite dimensional spaces used in the computations. It is just the order of

the space and the time derivatives appearing in the expressions which we need to take account of in addition to requiring conditions such as $U_1(0,t) = 0$ for our axisymmetric deformation.

For the $a(.;.)$ term appearing in (4.19)–(4.22) we require that the approximation $\underline{u} \approx \underline{U}$, with $\underline{u} = \underline{u}(r,t)$, satisfies

$$u_i(.,t) \in H^1(\Omega), \quad i = 1,3 \quad \text{and} \quad u_1(0,t) = 0 \tag{5.5}$$

and also satisfies the boundary conditions at $r = 1$. By considering the term $\nabla\underline{\psi}$ we similarly take test vectors such that

$$\psi_i(.,t) \in H^1(\Omega), \quad i = 1,3 \quad \text{and} \quad \psi_1(0,t) = \psi_1(1,t) = \psi_3(1,t) = 0. \tag{5.6}$$

The formulation of the dynamic problem appearing in (4.23)–(4.25) involves space derivatives and time derivatives and we now have $\underline{u} \approx \underline{U}$ and $\underline{v} \approx \underline{V}$. We take these approximations such that

$$u_i \in H^1((0,T), H^1(\Omega)), \quad v_i \in H^1((0,T), L_2(\Omega)), \quad i = 1,3 \quad \text{and} \quad u_1(0,t) = v_1(0,t) = 0 \tag{5.7}$$

and also that they satisfy appropriate boundary conditions at $r = 1$. (The notation used in (5.7) is standard, meaning that

$$u_i(.,t) \in H^1(\Omega), \quad v_i(.,t) \in L_2(\Omega), \quad u_i(r,.) \in H^1(0,T), \quad v_i(r,.) \in H^1(0,T), \quad i = 1,3.) \tag{5.8}$$

For the test vector $\underline{\psi}$ in this context we essentially have the same situation as in the quasi-static case, except that we now have to also consider the time dependence, and we take

$$\psi_i \in L_2((0,T), H^1(\Omega)), \quad i = 1,3, \quad \text{and} \quad \psi_1(0,t) = \psi_1(1,t) = \psi_3(1,t) = 0 \tag{5.9}$$

as there is no time dependence on $\underline{\psi}$ in the $A(.;.)$ expression in (4.24). The test vector $\underline{\theta}$ in (4.24) is just concerned with weakly imposing the condition that the velocity is the time derivative of the displacement and as the expression involves no space or time derivatives we just need

$$\theta_i \in L_2((0,T), L_2(\Omega)), \quad i = 1,3 \quad \text{with } \theta_1(0,t) = \theta_1(1,t) = \theta_3(1,t) = 0. \tag{5.10}$$

We actually restrict to functions $\theta_i \in L_2((0,T), H^1(\Omega)) \subset L_2((0,T), L_2(\Omega))$ in the implementation.

The test vectors $\underline{\psi}$ and $\underline{\theta}$ in the dynamic problem are the unknowns in the dual problem, which is derived from the dynamic problem, but they appear in a different way as the expressions were obtained using an integration by parts in time so that the expression that we use for $A'(.;.,.)$ involves first time derivatives on $\underline{\psi}$ and $\underline{\theta}$. Thus when we solve for $\underline{\psi}$ and $\underline{\theta}$ in the numerical scheme we need to be able to integrate the time derivatives of these and hence we take

$$\psi_i \in H^1((0,T), H^1(\Omega)), \quad i = 1,3, \quad \text{and} \quad \psi_1(0,t) = \psi_1(1,t) = \psi_3(1,t) = 0 \tag{5.11}$$

and we similarly we take

$$\theta_i \in H^1((0,T), H^1(\Omega)), \quad i = 1,3, \quad \text{and} \quad \theta_1(0,t) = \theta_1(1,t) = \theta_3(1,t) = 0. \tag{5.12}$$

In the dual problem it is the vectors labelled as $\underline{\alpha}$ and $\underline{\beta}$ which have the role of the test vectors and recall that in the derivation these are concerned with the directions in which we change $\underline{U}$ and $\underline{V}$ respectively when the Gateaux derivatives are obtained. Observe that there are no time derivatives on $\underline{\alpha}$ and $\underline{\beta}$ in (4.51). It thus follows that we can take

$$\alpha_i \in L_2((0,T),H^1(\Omega)), \quad i=1,3 \quad \text{and} \quad \alpha_1(0,t)=\alpha_1(1,t)=\alpha_3(1,t)=0 \tag{5.13}$$

and

$$\beta_i \in L_2((0,T),L_2(\Omega)), \quad i=1,3 \quad \text{and} \quad \beta_1(0,t)=\beta_1(1,t)=\beta_3(1,t)=0 \tag{5.14}$$

although in the computations we actually take $\beta_i \in L_2((0,T),H^1(\Omega)) \subset L_2((0,T),L_2(\Omega))$.

5.1.3 The piecewise polynomial approximations

We take piecewise polynomials for the approximations $\underline{u} \approx \underline{U}$ and $\underline{v} \approx \underline{V}$ and for the approximate solution $\underline{\psi}$, $\underline{\theta}$ in the dual problem. We have first time derivatives on the vectors $\underline{u}$, $\underline{v}$, $\underline{\psi}$ and $\underline{\theta}$ and thus we take functions which are continuous and piecewise linear in t with respect to the time levels $0=t_0<t_1<\cdots<t_N$. We similarly have first derivatives with respect to r on both components of the first three vectors and thus for these vectors we take functions which are continuous and piecewise polynomial in r with respect to the mesh points $0=r_0<r_1<\cdots<r_{\tilde{M}}=1$. We also take the same form for $\underline{\theta}$. For some detail, we let $H_1,\cdots,H_M$ denote the spatial basis functions so that at any time level $t=t_j$ we have

$$\underline{u}(r,t_j)=\underline{u}^j(r):=\sum_{i=1}^{M}\underline{u}_i^j H_i(r), \quad \underline{v}(r,t_j)=\underline{v}^j(r):=\sum_{i=1}^{M}\underline{v}_i^j H_i(r), \tag{5.15}$$

and similarly when we consider the dual problem

$$\underline{\psi}(r,t_j)=\underline{\psi}^j(r):=\sum_{i=1}^{M}\underline{\psi}_i^j H_i(r), \quad \underline{\theta}(r,t_j)=\underline{\theta}^j(r):=\sum_{i=1}^{M}\underline{\theta}_i^j H_i(r). \tag{5.16}$$

(The number of basis functions M depends on the number of elements $\tilde{M}$ and the degree of the polynomials used, e.g. $M=\tilde{M}+1$ for linears, $M=2\tilde{M}+1$ for quadratics etc..) Between time levels, i.e. $t_{j-1}<t<t_j$ we assume that

$$\underline{u}(r,t) = \left(\frac{t_j-t}{t_j-t_{j-1}}\right)\underline{u}^{j-1}(r)+\left(\frac{t-t_{j-1}}{t_j-t_{j-1}}\right)\underline{u}^j(r), \tag{5.17}$$

$$\underline{v}(r,t) = \left(\frac{t_j-t}{t_j-t_{j-1}}\right)\underline{v}^{j-1}(r)+\left(\frac{t-t_{j-1}}{t_j-t_{j-1}}\right)\underline{v}^j(r), \tag{5.18}$$

$$\underline{\psi}(r,t) = \left(\frac{t_j-t}{t_j-t_{j-1}}\right)\underline{\psi}^{j-1}(r)+\left(\frac{t-t_{j-1}}{t_j-t_{j-1}}\right)\underline{\psi}^j(r), \tag{5.19}$$

$$\underline{\theta}(r,t) = \left(\frac{t_j-t}{t_j-t_{j-1}}\right)\underline{\theta}^{j-1}(r)+\left(\frac{t-t_{j-1}}{t_j-t_{j-1}}\right)\underline{\theta}^j(r). \tag{5.20}$$

The time derivatives of $\underline{u}$, $\underline{v}$ and $\underline{\psi}$ are defined for $t_{j-1} < t < t_j$ and are given by

$$\underline{\dot{u}}(r,t) = \frac{1}{t_j - t_{j-1}} \left(\underline{u}^j(r) - \underline{u}^{j-1}(r) \right), \tag{5.21}$$

$$\underline{\dot{v}}(r,t) = \frac{1}{t_j - t_{j-1}} \left(\underline{v}^j(r) - \underline{v}^{j-1}(r) \right), \tag{5.22}$$

$$\underline{\dot{\psi}}(r,t) = \frac{1}{t_j - t_{j-1}} \left(\underline{\psi}^j(r) - \underline{\psi}^{j-1}(r) \right), \tag{5.23}$$

$$\underline{\dot{\theta}}(r,t) = \frac{1}{t_j - t_{j-1}} \left(\underline{\theta}^j(r) - \underline{\theta}^{j-1}(r) \right). \tag{5.24}$$

These time derivatives are piecewise constant in time.

5.2 The quasi-static problem

In the computational scheme for the quasi-static problem we determine the displacement $\underline{u}^j(r)$ at each time level which satisfies

$$a(\underline{u}^j; \underline{\psi}) = F(\underline{\psi}) \quad \text{for all } \underline{\psi} \in S_h, \tag{5.25}$$

where S_h is an appropriate subspace of

$$\text{span} \left\{ \begin{pmatrix} H_1 \\ 0 \end{pmatrix}, \begin{pmatrix} 0 \\ H_1 \end{pmatrix}, \begin{pmatrix} H_2 \\ 0 \end{pmatrix}, \begin{pmatrix} 0 \\ H_2 \end{pmatrix}, \cdots \begin{pmatrix} H_M \\ 0 \end{pmatrix}, \begin{pmatrix} 0 \\ H_M \end{pmatrix} \right\}. \tag{5.26}$$

The only test vectors which are not used are those attached to displacement degrees of freedom which are known corresponding to the points $r = 0$ and $r = 1$. (5.25) gives a nonlinear system in the nodal parameters of $\underline{u}^j$ which are unknown. Let $(\underline{u}^j)^{(k)}$, $k = 0, 1, 2, \cdots$ denote the functions corresponding to each Newton iteration in the attempt to solve (5.25) and we write instead $a((\underline{u}^j)^{(k)}, P(t_j); \underline{\psi})$ for $a((\underline{u}^j)^{(k)}; \underline{\psi})$ to make clearer that the form changes with j. As already indicated a possible starting iterate is $(\underline{u}^j)^{(0)} = \underline{u}^{j-1}$ and subsequent iterates are determined so that

$$a((\underline{u}^j)^{(k)}, P(t_j); \underline{\psi}) + a'((\underline{u}^j)^{(k)}, P(t_j); (\underline{u}^j)^{(k+1)} - (\underline{u}^j)^{(k)}, \underline{\psi}) = F(\underline{\psi}) \quad \text{for all } \underline{\psi} \in S_h. \tag{5.27}$$

This is a linear system for the change $(\underline{u}^j)^{(k+1)} - (\underline{u}^j)^{(k)}$ in the iterates and the linear system has a matrix, the Jacobian matrix, which is symmetric because of the symmetry property of $a'((\underline{u}^j)^{(k)}, P(t_j); ., .)$ discussed in subsection 4.2. If this Newton iteration fails to converge with the loading $P(t_j)$ then we can change t_j to be closer to t_{j-1} at which we already have a solution. This modification of reducing the time step will eventually lead to a convergent iteration provided we are not at or very close to critical points as at critical points the Jacobian matrix is singular.

5.3 The dynamic problem

The approximate dynamic solution at time t_j involves determining $\underline{u}^j$ and $\underline{v}^j$ satisfying an equation of the form

$$A(\begin{pmatrix} \underline{u}^j \\ \underline{v}^j \end{pmatrix}, P(t_j); \begin{pmatrix} \underline{\psi} \\ \underline{\theta} \end{pmatrix}) = F(\begin{pmatrix} \underline{\psi} \\ \underline{\theta} \end{pmatrix}), \quad \text{for all } \underline{\psi} \in S_h^d, \quad \underline{\theta} \in S_h^d, \tag{5.28}$$

where S_h^d is an appropriate space constructed using the functions $H_1, \cdots, H_M$ to describe the spatial dependence. As the test functions only need to be such that $\underline{\psi}(r,.) \in L_2((0,T))$ and $\underline{\theta}(r,.) \in L_2((0,T))$ we can choose them to be non-zero only on one time interval at each stage and in this way the equations we solve at time t_j only involve the solution already obtained at one previous time level, i.e. at t_{j-1}.

To get started we need the solution at the initial time $t_0 = 0$ and this is obtained by projecting the initial displacement $\underline{U}^0$ and the initial velocity $\underline{V}^0$ into the approximating space in the sense that $\underline{u}^0$ and $\underline{v}^0$ satisfy

$$\int_0^1 \underline{u}^0(r) \cdot \underline{\theta}\, r \mathrm{d}r = \int_0^1 \underline{U}^0(r) \cdot \underline{\theta}\, r \mathrm{d}r, \quad \int_0^1 \underline{v}^0(r) \cdot \underline{\psi}\, r \mathrm{d}r = \int_0^1 \underline{V}^0(r) \cdot \underline{\psi}\, r \mathrm{d}r \quad \text{for all } \underline{\psi}, \underline{\theta} \in S_h^d. \tag{5.29}$$

This gives linear systems involving mass matrices. Note that for a simple initial condition such as a pre-stretch state corresponding to $\underline{U}^0 = (\gamma r, 0)^T$ we have $\underline{U}^0 \in \hat{S}^h$ and hence in this case we simply have $\underline{u}^0 = \underline{U}^0$. In some of the examples, this projection is however necessary to generate the initial velocity vector.

We consider next how to determine the solution at time t_j for $j \geq 1$. Now whatever choice is made for $\underline{\psi}$ and $\underline{\theta}$ we have equations of the form

$$\int_{t_{j-1}}^{t_j} \int_0^1 \rho h_0 (\dot{\underline{u}} - \underline{v}) \cdot \underline{\theta}\, r \mathrm{d}r \mathrm{d}t = 0 \quad \text{for all appropriate } \underline{\theta}, \tag{5.30}$$

$$\int_{t_{j-1}}^{t_j} \int_0^1 r \left(\tilde{a}_1(\underline{u}(r,t); \underline{\psi}(r,t)) - P(t) \tilde{a}_2(\underline{u}(r,t); \underline{\psi}(r,t)) + \rho h_0 \dot{\underline{v}}(r,t) \cdot \underline{\psi} \right) \mathrm{d}r \mathrm{d}t = 0$$
$$\text{for all appropriate } \underline{\psi}. \tag{5.31}$$

We get different schemes for different choices of the time dependence of $\underline{\theta}$ and $\underline{\psi}$ with in all cases a quadrature needed to approximate the time integral in (5.31). We just describe one possibility here in which we take $\underline{\psi}$ and $\underline{\theta}$ to be constant in time on (t_{j-1}, t_j) and for the quadrature in time we use the mid-point rule. This gives us

$$(t_j - t_{j-1}) \int_0^1 \left(\tilde{a}_1(\underline{u}^{j-1/2}; \underline{\psi}) - P(t_{j-1/2}) \tilde{a}_2(\underline{u}^{j-1/2}; \underline{\psi}) + \frac{\rho h_0}{t_j - t_{j-1}} (\underline{v}^j - \underline{v}^{j-1}) \right) \cdot \underline{\psi})\, r \mathrm{d}r = 0 \tag{5.32}$$

where

$$t_{j-1/2} = \frac{t_{j-1} + t_j}{2} \tag{5.33}$$

and where

$$\underline{u}^{j-1/2} = \frac{1}{2}(\underline{u}^{j-1} + \underline{u}^j) = \frac{1}{2} \sum_1^M (\underline{u}_k^{j-1} + \underline{u}_k^j) N_k(r). \tag{5.34}$$

To be able to obtain an equation involving only $\underline{u}^j$ we need to express $\underline{v}^j$ in terms of $\underline{u}^j$ by making use of (5.30).

As already stated, our choice is that $\underline{\theta}$ is independent of t and we have

$$\int_0^1 \left((\underline{u}^j - \underline{u}^{j-1}) - \frac{1}{2}(t_j - t_{j-1})(\underline{v}^{j-1} + \underline{v}^j) \right) \cdot \underline{\theta}\, r \mathrm{d}r = 0 \quad \text{for all appropriate } \underline{\theta} \in S_h^d. \tag{5.35}$$

Now since

$$(\underline{u}^j - \underline{u}^{j-1}) - \frac{1}{2}(t_j - t_{j-1})(\underline{v}^{j-1} + \underline{v}^j) \in S_h^d \tag{5.36}$$

it follows that

$$\underline{u}^j - \underline{u}^{j-1} = \frac{1}{2}(t_j - t_{j-1})(\underline{v}^{j-1} + \underline{v}^j) \tag{5.37}$$

giving

$$\underline{v}^j = \frac{2}{t_j - t_{j-1}}(\underline{u} - \underline{u}^{j-1}) - \underline{v}^{j-1} \tag{5.38}$$

and the acceleration term is given by

$$\frac{\underline{v}^j - \underline{v}^{j-1}}{t_j - t_{j-1}} = \frac{2}{t_j - t_{j-1}}\left(\frac{\underline{u}^j - \underline{u}^{j-1}}{t_j - t_{j-1}} - \underline{v}^{j-1}\right). \tag{5.39}$$

Substituting into (5.32) gives, after dividing by $t_j - t_{j-1}$,

$$\begin{aligned}\int_0^1 \Big\{ &\tilde{a}_1(\underline{u}^{j-1/2}; \underline{\psi}) - P(t_{j-1/2})\tilde{a}_2(\underline{u}^{j-1/2}; \underline{\psi}) \\ &+ \frac{2\rho h_0}{t_j - t_{j-1}}\left(\frac{\underline{u}^j - \underline{u}^{j-1}}{t_j - t_{j-1}} - \underline{v}^{j-1}\right) \cdot \underline{\psi} \Big\} r \mathrm{d}r = 0 \\ &\text{for all appropriate } \underline{\psi} \in S_h^d.\end{aligned}$$

This is similar in form to (5.25) in the quasi-static case except that here the pressure is evaluated at the mid-time $t_{j-1/2}$ and we have the extra inertia term. The Newton iteration that we use to solve this equation is also similar to the quasi-static case. If we write the equations in the form

$$g(\underline{u}^j; \underline{\psi}) = 0 \quad \text{for all appropriate } \underline{\psi} \in S_h^d \tag{5.40}$$

then the Newton iteration for solving this involves iterates computed from

$$g((\underline{u}^j)^{(k)}; \underline{\psi}) + g'((\underline{u}^j)^{(k)}; (\underline{u}^j)^{(k+1)} - (\underline{u}^j)^{(k)}, \underline{\psi}) = 0. \tag{5.41}$$

If we let $\underline{y} = (\underline{u}^j)^{(k+1)} - (\underline{u}^j)^{(k)}$ and let $(\underline{u}^{j-1/2})^{(k)} = (\underline{u}^{j-1} + (\underline{u}^j)^{(k)})$ then the Gateaux derivative of g is given by

$$\begin{aligned}g'((\underline{u}^j)^{(k)}; \underline{y}, \underline{\psi}) \quad = \quad &\int_0^1 \Big\{ \frac{1}{2}\Big(\tilde{a}_1'((\underline{u}^{j-1/2})^{(k)}; \underline{y}, \underline{\psi}) - P(t_{j-1/2})\tilde{a}_2'((\underline{u}^{j-1/2})^{(k)}; \underline{y}, \underline{\psi}) \Big) \\ &+ \frac{2\rho h_0}{(t_j - t_{j-1})^2}\underline{y} \cdot \underline{\psi} \Big\} r \mathrm{d}r\end{aligned} \tag{5.42}$$

which should be compared to the corresponding term $a'((\underline{u}^j)^{(k)}; \underline{y}, \underline{\psi})$ in the quasi-static scheme. The procedure thus involves solving this nonlinear equation for $\underline{u}^j$ by Newton's method and setting

$$\underline{v}^j = \frac{2}{t_j - t_{j-1}}(\underline{u}^j - \underline{u}^{j-1}) - \underline{v}^{j-1}. \tag{5.43}$$

As in the quasi-static case, the linear system associated with these equations has a symmetric matrix.

5.4 The dual problem

To approximately solve the dual problem (4.74)–(4.75) we must already have an approximation $\underline{u} \approx \underline{U}$ available which in this application could be an approximation to the solution of the dynamic problem, from which the dual problem is derived, or it could even be an approximation obtained by neglecting inertia effects throughout. Note that as the the expressions explicitly involve the final time $t_N = T$ the solution procedure must be backward in time involving first determining $\underline{\psi}(.,T)$ and $\underline{\theta}(.,T)$ and then determining $\underline{\psi}(.,t_j)$ and $\underline{\theta}(.,t_j)$ for $j = N-1, N-2, \cdots, 1, 0$. In the description we let S_h^D denote the appropriate subspace of

$$\text{span}\left\{\begin{pmatrix} H_1 \\ 0 \end{pmatrix}, \begin{pmatrix} 0 \\ H_1 \end{pmatrix}, \begin{pmatrix} H_2 \\ 0 \end{pmatrix}, \begin{pmatrix} 0 \\ H_2 \end{pmatrix}, \cdots \begin{pmatrix} H_M \\ 0 \end{pmatrix}, \begin{pmatrix} 0 \\ H_M \end{pmatrix}\right\} \tag{5.44}$$

in which each function $\underline{\psi}^j(r)$ and $\underline{\theta}^j(r)$ lie.

5.4.1 The final time $t = t_N = T$: determining $\underline{\psi}^N(r)$ and $\underline{\theta}^N(r)$

Our discretization of (4.74)–(4.75) is to take

$$(\underline{\alpha}, \underline{\theta}^N)_\Omega = \int_0^1 (\underline{\alpha}(r) \cdot \underline{J}_\alpha(r,T) + \underline{\alpha}'(r) \cdot \underline{J}_{\alpha'}(r,T))\, r\mathrm{d}r, \quad \text{for all } \underline{\alpha} \in S^h, \tag{5.45}$$

$$(\underline{\beta}, \underline{\psi}^N)_\Omega, = \int_0^1 (\underline{\beta} \cdot \underline{J}_\beta(r,T) + \underline{\beta}' \cdot \underline{J}_{\beta'}(r,T))\, r\mathrm{d}r, \quad \text{for all } \underline{\beta} \in S_h^D. \tag{5.46}$$

Both of these involve linear systems with mass matrices. This step is similar to the step of obtaining $\underline{u}^0$ and $\underline{v}^0$ in the dynamic problem.

5.4.2 At time $t = t_j$, $j < N$: determining $\underline{\psi}^j(r)$ and $\underline{\theta}^j(r)$

As with the dynamic problem we can choose the test vectors ($\underline{\alpha}$ and $\underline{\beta}$ in this case) to be non-zero only on one time interval and thus we have

$$-\rho h_0 \int_{t_j}^{t_{j+1}} \int_0^1 \left(\frac{1}{t_{j+1}-t_j}(\underline{\psi}^{j+1} - \underline{\psi}^j) + \underline{\theta}\right) \cdot \underline{\beta}\, r\mathrm{d}r\mathrm{d}t = \int_{t_j}^{t_{j+1}} \int_0^1 (\underline{\beta} \cdot \underline{J}_\beta + \underline{\beta}' \cdot \underline{J}_{\beta'})\, r\mathrm{d}r\mathrm{d}t \tag{5.47}$$

and

$$\int_{t_j}^{t_{j+1}} \int_0^1 \left(\tilde{a}_1'(\underline{u}(r,t); \underline{\alpha}, \underline{\psi}) - P(t)\tilde{a}_1'(\underline{u}(r,t); \underline{\alpha}, \underline{\psi}) - \rho h_0 \underline{\alpha} \cdot \dot{\underline{\theta}}\right) r\mathrm{d}r\mathrm{d}t$$
$$= \int_{t_j}^{t_{j+1}} \int_0^1 (\underline{\alpha} \cdot \underline{J}_\alpha + \underline{\alpha}' \cdot \underline{J}_{\alpha'})\, r\mathrm{d}r\mathrm{d}t. \tag{5.48}$$

These resemble in form equations (5.30) and (5.31) in the dynamic problem and we again have the situation in which different choices of the time dependence of the test functions gives us different schemes. We follow a similar approach to that used in the dynamic scheme and we present one scheme here corresponding to the case that $\underline{\alpha}$ and $\underline{\beta}$ are both

constant on each time interval (t_j, t_{j+1}) and we approximate the time integrals by quadrature and using the mid-point rule. This gives

$$\begin{aligned}
&(t_{j+1}-t_j)\int_0^1 \left(\tilde{a}_1'(\underline{u}^{j+1/2};\underline{\alpha},\underline{\psi}^{j+1/2}) - P(t_{j+1/2})\tilde{a}_2'(\underline{u}^{j+1/2};\underline{\alpha},\underline{\psi}^{j+1/2})\right) r\mathrm{d}r \\
&\qquad -\rho h_0 \int_0^1 \underline{\alpha}\cdot\left(\frac{\underline{\theta}^{j+1}-\underline{\theta}^j}{t_{j+1}-t_j}\right) r\mathrm{d}r \\
= \;& (t_{j+1}-t_j)\int_0^1 \left(\underline{\alpha}\cdot\underline{J}_\alpha(\underline{u}^{j+1/2}) + \underline{\alpha}'\cdot\underline{J}_{\alpha'}(\underline{u}^{j+1/2})\right) r\mathrm{d}r \quad \text{for all } \underline{\alpha}\in S_h^D, \quad (5.49)
\end{aligned}$$

where

$$t_{j+1/2} = \frac{t_j + t_{j+1}}{2} \quad \text{and} \quad \underline{u}^{j+1/2}(r) = \underline{u}(r, t_{j+1/2}) \tag{5.50}$$

and where

$$\underline{\psi}^{j+1/2} = \frac{1}{2}(\underline{\psi}^j + \underline{\psi}^{j+1}) = \frac{1}{2}\sum_k \left((\underline{\psi}^j)_k + (\underline{\psi}^{j+1})_k\right) N_k(r) \in S_h^D. \tag{5.51}$$

In this case we need to use (5.47) to express $\underline{\theta}^j$ in terms of $\underline{\psi}^j$ so that we can get an equation which only involves $\underline{\psi}^j$ and the scheme that we get depends on the choice of $\underline{\beta}$ and we just restrict to the case that $\underline{\beta}$ is constant in time on (t_j, t_{j+1}). Then

$$\begin{aligned}
&-\rho h_0 \int_0^1 \left((\underline{\psi}^{j+1}-\underline{\psi}^j) + \frac{t_{j+1}-t_j}{2}(\underline{\theta}^j + \underline{\theta}^{j+1})\right)\cdot\underline{\beta}\, r\mathrm{d}r \\
&\qquad = (t_{j+1}-t_j)\int_0^1 (\underline{\beta}\cdot\underline{J}_\beta(\underline{u}^{j+1/2}) + \underline{\beta}'\cdot\underline{J}_{\beta'}(\underline{u}^{j+1/2}))\, r\mathrm{d}r \quad \text{for all } \underline{\beta}\in S_h^D. \quad (5.52)
\end{aligned}$$

To get the connection between $\underline{\psi}^j$ and $\underline{\theta}^j$ we let

$$\underline{\gamma}^j = (\underline{\psi}^{j+1}-\underline{\psi}^j) + \frac{t_{j+1}-t_j}{2}(\underline{\theta}^j + \underline{\theta}^{j+1}) = \sum_{k=1}^{M-1} \underline{\gamma}_k^j N_k(r) \in S_h^D \tag{5.53}$$

so that

$$-\rho h_0 \int_0^1 \underline{\gamma}^j\cdot\underline{\alpha}\, r\mathrm{d}r = (t_{j+1}-t_j)\int_0^1 (\underline{\beta}\cdot\underline{J}_\beta(\underline{u}^{j+1/2}) + \underline{\beta}'\cdot\underline{J}_{\beta'}(\underline{u}^{j+1/2}))\, r\mathrm{d}r \quad \text{for all } \underline{\beta}\in S_h^D. \tag{5.54}$$

This is a linear problem involving a mass matrix for the components $\underline{\gamma}_k^j$ which are unknown. Once these are obtained we have the functions $\underline{\gamma}^j$ and

$$\underline{\theta}^j = -\underline{\theta}^{j+1} + \frac{2}{t_{j+1}-t_j}\left(\underline{\gamma}^j - (\underline{\psi}^{j+1}-\underline{\psi}^j)\right) \tag{5.55}$$

which gives

$$\begin{aligned}
\dot{\underline{\theta}} &= \frac{1}{t_{j+1}-t_j}(\underline{\theta}^{j+1}-\underline{\theta}^j) && (5.56)\\
&= \frac{2}{t_{j+1}-t_j}\left(\underline{\theta}^{j+1} - \frac{1}{t_{j+1}-t_j}(\underline{\gamma}^j - (\underline{\psi}^{j+1}-\underline{\psi}^j))\right) && (5.57)\\
&= \frac{-2}{(t_{j+1}-t_j)^2}\underline{\gamma}^j + \frac{2}{t_{j+1}-t_j}\left(\underline{\theta}^{j+1} + \frac{1}{(t_{j+1}-t_j)}(\underline{\psi}^{j+1}-\underline{\psi}^j)\right). && (5.58)
\end{aligned}$$

Substituting into (5.49) gives the system for $\underline{\psi}^j$, i.e. we have

$$\begin{aligned}
&(t_{j+1}-t_j)\int_0^1 \left(\tilde{a}_1'(\underline{u}^{j+1/2};\underline{\alpha},\underline{\psi}^{j+1/2}) - P(t_{j+1/2})\tilde{a}_2'(\underline{u}^{j+1/2};\underline{\alpha},\underline{\psi}^{j+1/2})\right) r\mathrm{d}r \\
&\qquad -2\rho h_0\int_0^1 \underline{\alpha}\cdot\left(\frac{-1}{(t_{j+1}-t_j)}\underline{\gamma}^j + (\underline{\theta}^{j+1} + \frac{1}{(t_{j+1}-t_j)}(\underline{\psi}^{j+1}-\underline{\psi}^j))\right) r\mathrm{d}r \\
= \quad &(t_{j+1}-t_j)\int_0^1 \left(\underline{\alpha}\cdot\underline{J}_\alpha(\underline{u}^{j+1/2}) + \underline{\alpha}'\cdot\underline{J}_{\alpha'}(\underline{u}^{j+1/2})\right) r\mathrm{d}r \quad \text{for all } \underline{\alpha}\in S_h^D. \quad (5.59)
\end{aligned}$$

Collecting together the $\underline{\psi}^j$ terms on the left hand side and the known terms on the right hand side gives

$$\begin{aligned}
&\frac{(t_{j+1}-t_j)}{2}\int_0^1 \left(\tilde{a}_1'(\underline{u}^{j+1/2};\underline{\alpha},\underline{\psi}^j) - P(t_{j+1/2})\tilde{a}_2'(\underline{u}^{j+1/2};\underline{\alpha},\underline{\psi}^j)\right) r\mathrm{d}r \\
&\qquad +\frac{2\rho h_0}{(t_{j+1}-t_j)}\int_0^1 \underline{\alpha}\cdot\underline{\psi}^j\, r\mathrm{d}r \\
= \quad &-\frac{(t_{j+1}-t_j)}{2}\int_0^1 \left(\tilde{a}_1'(\underline{u}^{j+1/2};\underline{\alpha},\underline{\psi}^{j+1}) - P(t_{j+1/2})\tilde{a}_2'(\underline{u}^{j+1/2};\underline{\alpha},\underline{\psi}^{j+1})\right) r\mathrm{d}r \\
&\quad -\frac{2\rho h_0}{(t_{j+1}-t_j)}\int_0^1 \underline{\alpha}\cdot\underline{\gamma}^j\, r\mathrm{d}r + 2\rho h_0\int_0^1 \underline{\alpha}\cdot\left(\underline{\theta}^{j+1} - \frac{1}{(t_{j+1}-t_j)}\underline{\psi}^{j+1}\right) r\mathrm{d}r \\
&\qquad +(t_{j+1}-t_j)\int_0^1 \left(\underline{\alpha}\cdot\underline{J}_\alpha(\underline{u}^{j+1/2}) + \underline{\alpha}'\cdot\underline{J}_{\alpha'}(\underline{u}^{j+1/2})\right) r\mathrm{d}r, \qquad (5.60)
\end{aligned}$$

for all $\underline{\alpha}\in S_h^D$. As the expression on the left of the equal sign is symmetric in $\underline{\alpha}$ and $\underline{\psi}^j$ we get a linear system with a symmetric matrix to determine the coefficients of $\underline{\psi}^j$. Once these are obtained we obtain the coefficients of $\underline{\theta}^j$ using (5.55).

5.5 Using the dual solution to adaptively refine a mesh

As already stated a few times, the theory described in this report leading to the estimate

$$J(U) - J(u_h) \approx F(z) - A(u_h; z_h) \qquad (5.61)$$

of the error in approximating a QoI $J(U)$ by $J(u_h)$ is applicable whatever the source of the error, i.e. discretization error, modelling error or both. When there is modelling error repeatedly refining the meshes used to obtain u_h and z_h becomes pointless as $F(z_h) - A(u_h; z_h) \not\to 0$ but instead converges to the modelling error alone. In this situation we would just wish to refine until two approximations of this estimate are about the same. However, when we only have discretization error we do have $F(z_h) - A(u_h; z_h) \to 0$ as $h \to 0$ and we can make further use of z_h to determine how we should adaptively refine a mesh so that we can make $|F(z_h) - A(u_h; z_h)|$ less than a desired tolerance. We consider now how this can be done to adapt a space mesh when we just have the quasi-static problem to consider.

In the quasi-static case the exact displacement $\underline{U}$ satisfies

$$a(\underline{U};\underline{\psi}) = 0 \quad \text{for all appropriate } \underline{\psi} \qquad (5.62)$$

(see (4.19), i.e. the $F(.)$ term is 0) and the approximate displacement $\underline{u}_h$ satisfies

$$a(\underline{u}_h;\underline{\psi}) = 0 \quad \text{for all appropriate } \underline{\psi} \text{ in } V_h. \qquad (5.63)$$

The dual solution in this case is denoted by $\underline{\psi}_h$ which we assume is in a space $\hat{V}_h$ which contains the finite element test space V_h. The estimate is now

$$J(\underline{U}) - J(\underline{u}_h) \approx -a(\underline{u}_h, \underline{\psi}_h) = -a(\underline{u}_h, \underline{\psi}_h - \pi\underline{\psi}_h) \tag{5.64}$$

$$= -\sum_{k=1}^{m} a(\underline{u}_h, \underline{\psi}_h - \pi\underline{\psi}_h)_k \tag{5.65}$$

where $\pi\underline{\psi}_h \in V_h$ is the nodal interpolant of $\underline{\psi}_h \in \hat{V}_h$ and where $\tilde{M}$ is the number of elements. The element quantity $a(\underline{u}_h, \underline{\psi}_h - \pi\underline{\psi}_h)_k$ gives an indication of the error in the kth element, $k = 1, 2, \cdots, \tilde{M}$. If the aim of the computation is to compute $\underline{u}_h$ such that $|J(\underline{U}) - J(\underline{u}_h)| \leq \delta$ then this is most economically just achieved if we have

$$|a(\underline{u}_h, \underline{\psi}_h - \pi\underline{\psi}_h)_k| \approx \frac{\delta}{\tilde{M}}, \quad k = 1, 2, \cdots, \tilde{M}. \tag{5.66}$$

If the element quantity for the kth element is larger than $\delta/\tilde{M}$ then we opt to refine the kth element. To determine by how much we should divide the kth element we consider what is needed if we are in the asymptotic convergence range. If we are using degree p polynomials then dividing the element into q_k equal parts should decrease the quantity corresponding to the region of the kth element by a factor of about q_k^{2p}. This suggests that we select q_k so that

$$q_k^{2p} \approx \frac{|a(\underline{u}_h, \underline{\psi}_h - \pi\underline{\psi}_h)_k|}{\delta/\tilde{M}} > 1. \tag{5.67}$$

In fact it is usually beneficial to take a slightly larger value than this as otherwise a strategy of aiming to almost exactly get to the required accuracy often results in a new mesh which which has an error which is slightly larger than δ. If the value obtained for q_k selected by the above is large then it is also beneficial to replace it by some fixed value with the knock on effect that more than one mesh refinement will be needed before the accuracy of δ is obtained.

The mesh adaption procedure used is as follows.

1. We solve on a mesh of $\tilde{M}$ elements and compute the quantities $a(\underline{u}_h, \underline{\psi}_h - \pi\underline{\psi}_h)_k$, $k = 1, 2, \cdots, \tilde{M}$.

2. If
$$\left| \sum_{k=1}^{\tilde{M}} a(\underline{u}_h, \underline{\psi}_h - \pi\underline{\psi}_h)_k \right| \leq \delta \tag{5.68}$$
then we stop the computation.

3. For $k = 1, 2, \cdots, \tilde{M}$ we test as follows.

   If
   $$|a(\underline{u}_h, \underline{\psi}_h - \pi\underline{\psi}_h)_k| < \frac{\delta}{\tilde{M}} \tag{5.69}$$
   then we set $q_k = 1$ and goto the next value of k.

Otherwise we compute

$$q_k = \texttt{ceil}\left(\frac{1.05\left|a(\underline{u}_h, \underline{\psi}_h - \pi\underline{\psi}_h)_k\right|}{\delta/\tilde{M}}\right)^{1/(2p)}. \tag{5.70}$$

If $q_k > 16$ then we re-set $q_k = 16$.
We divide the kth element into q_k parts.

4. We replace $\tilde{M}$ by $q_1 + q_2 + \cdots + q_{\tilde{M}}$ and goto step 1.

The factor of 1.05 and the bound of 16 used above were arbitrarily selected. These values work reasonably well in the test problems considered although other values close to these are also likely to work well.

6 Results: discretization error

In this section we test the procedure in the case when the error in estimating a QoI is just due to discretization error. The physical problem that we are considering is the nonlinear problem of the inflation of a hyperelastic membrane introduced in section 4. We consider the following two quantities of interest:

$$J_1(\underline{U}) = \psi(\underline{U}) = \int_0^1 \tilde{\psi}\,\mathrm{d}r, \quad \tilde{\psi} = h_0 r W - \frac{P}{3}(r+u_1)\left(-(r+u_1)u_3' + (1+u_1')u_3\right), \tag{6.1}$$

which is the total potential energy, and

$$J_2(\underline{U}) = \frac{2}{b^2}\int_0^b r\lambda_3(r)\,\mathrm{d}r \tag{6.2}$$

which is a measure of the thickness ratio λ_3 in the vicinity of the pole at $r = 0$. We take $b = 1/8$ in the computations. $r = b$ is a node on each of the meshes used.

To be specific for the computations, we use a strain energy function W of the Mooney-Rivlin form given by

$$W = \frac{1}{2}\left(\lambda_1^2 + \lambda_2^2 + \lambda_3^2 - 3\right) + \frac{0.1}{2}\left(\lambda_1^{-2} + \lambda_2^{-2} + \lambda_3^{-2} - 3\right) \tag{6.3}$$

where, as before, λ_1 and λ_2 are the principal stretch ratios tangential to the mid-surface and where $\lambda_3 = 1/(\lambda_1\lambda_2)$ is the stretch ratio through the thickness. As the results only depend on the ratio P/h_0, where P is the applied pressure and h_0 is the undeformed thickness, we have taken $h_0 = 1$ in our computations.

Before we consider estimating $J_1(\underline{U})$ and $J_2(\underline{U})$ we show graphically various features of the solution. In figures 6.1 and 6.2 we show the deformed membranes at a selection of increasing pressures. These plots depend on $\underline{U}$. In figures 6.3 and 6.4 we show the stretch ratios λ_1, λ_2 and λ_3 at the selection of pressures. These plots depend on $\underline{U}'$. The plots suggest a 'fairly smooth' solution with not too great a variation in the quantities shown over the domain $0 \le r \le 1$. This is confirmed in the results as the meshes selected are never too far from being uniform. However, as we demonstrate, the theory still enables

us to predict $J(\underline{U}) - J(\underline{u}_h)$ accurately and to show how to re-mesh to achieve the required accuracy in a small number of steps.

In tables 6.1–6.11 we show results obtained for estimating the total potential energy in the case of $P = 1$ (in tables 6.1–6.5) and in the case of $P = 3$ (in tables 6.6–6.11). For each pressure P we consider a finite element space V_h corresponding to linears, quadratics and cubics and in most cases we consider the effect of both uniformly refining and adaptively refining. In all the tables m denotes the number of elements and $-a(\underline{u}_h, \underline{\hat{\psi}}_h)$ is the error estimate. As described in section 5.1.3, the space $\tilde{V}_h$ involves piecewise polynomials of one degree higher than that which is used for V_h. In all cases the so-called 'exact-error' is obtained by using the finite element solution with 1024 quadratic element as effectively the exact solution.

In all the tables, the ratio of the error estimate and the exact error are very close to 1 which is consistent with the asymptotic exactness described in section 3.7. The adaptive results described in tables 6.2 and 6.4 (for $P = 1$) and in tables 6.7, 6.9 and 6.11 (for $P = 3$) indicate how well the error estimation and adapting procedure works to achieve the desired accuracy in a small number of steps. In all cases, even for the coarsest mesh of 8 elements, we appear to be within the region where the asymptotic rate of convergence is in effect. The smoothness of the solution is evident by how rapidly the approximations converge when the quadratic and cubic elements are used.

A similar batch of results is obtained when $J(\underline{U}) = J_2(\underline{U})$ and we show these in tables 6.12–6.17.

In all the above cases the adaptive procedure selects a mesh which is fairly uniform. As a final test we consider the case of a non-homogeneous material corresponding to the strain energy function

$$W = C(r)\left\{\frac{1}{2}\left(\lambda_1^2 + \lambda_2^2 + \lambda_3^2 - 3\right) + \frac{0.1}{2}\left(\lambda_1^{-2} + \lambda_2^{-2} + \lambda_3^{-2} - 3\right)\right\} \tag{6.4}$$

with

$$C(r) = 1 - 0.9r, \quad 0 \le r \le 1. \tag{6.5}$$

This describes a Mooney Rivlin material which is stiffer at the centre (where $C(0) = 1$) than at the edge (where $C(1) = 0.1$). The profiles and material paths in this case for pressures up to $P = 1$ are shown in figure 6.5. There is now much more tangential stretching at the edge corresponding to $r = 1$. With quadratic elements and a QoI which is the total potential energy we show in figure 6.6 the variation of the mesh size (on a log scale) with r, $0 \le r < 1$, that the procedure generates to achieve an accuracy of 10^{-10} starting from a uniform mesh of 8 elements. Observe that in the final mesh of 299 quadratic elements the elements near $r = 1$ are about $1/20$th of the width of those near to the centre at $r = 0$. Table 6.18 shows the error estimates generated by the adaptive procedure and this should be compared with table 6.19 which shows what happens when we just perform a sequence of uniform refinements.

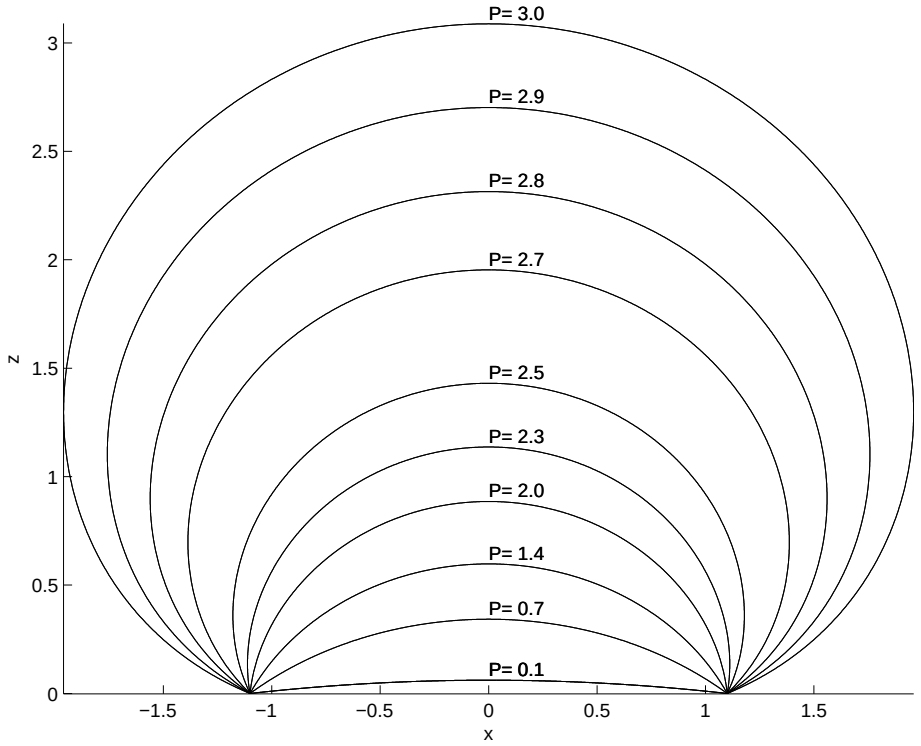

Figure 6.1: Profiles of a cross section of the deformed membranes at different pressures P.

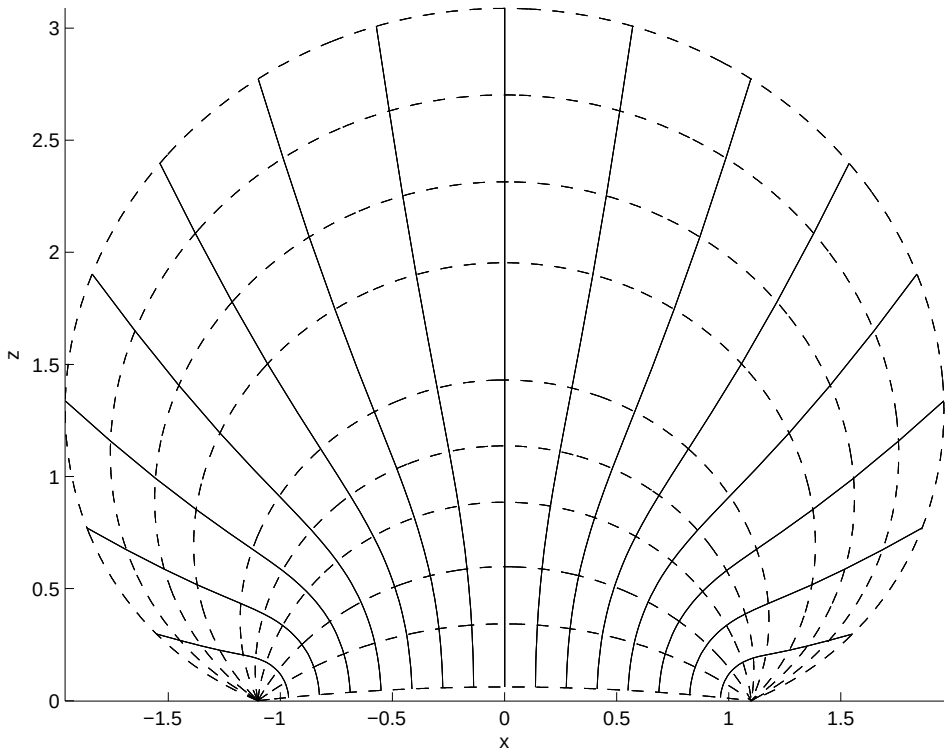

Figure 6.2: The paths of selected points as the membrane deforms as the pressure P increases (solid lines) together with the profiles shown in figure 6.1 (dashed lines).

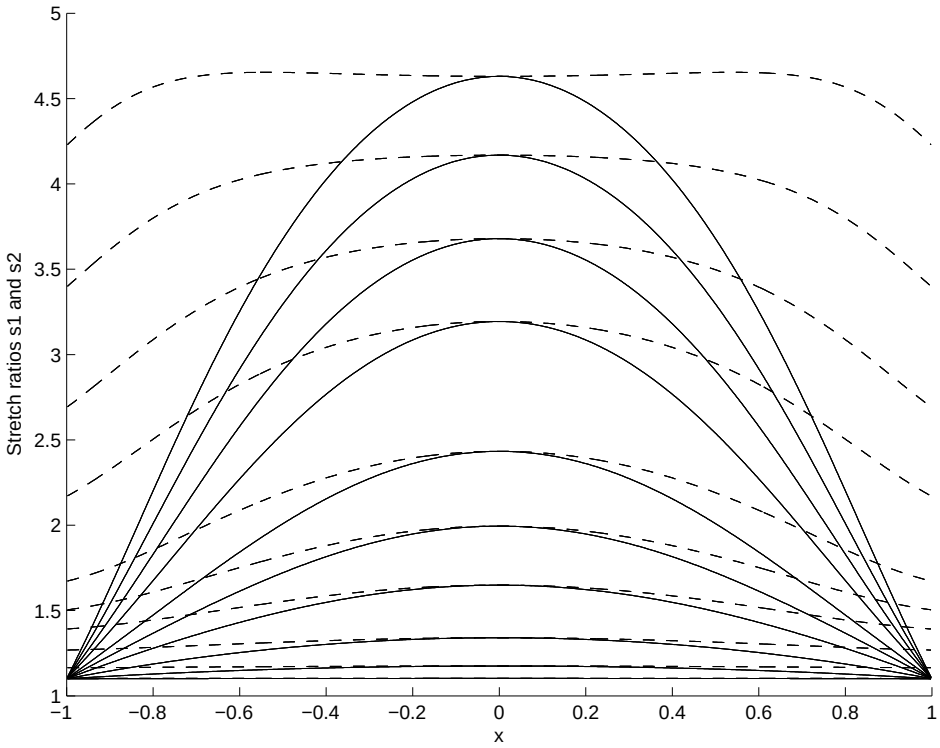

Figure 6.3: Stretch ratios λ_1 (dashed line) and λ_2 (solid line) for the profiles of figure 6.1.

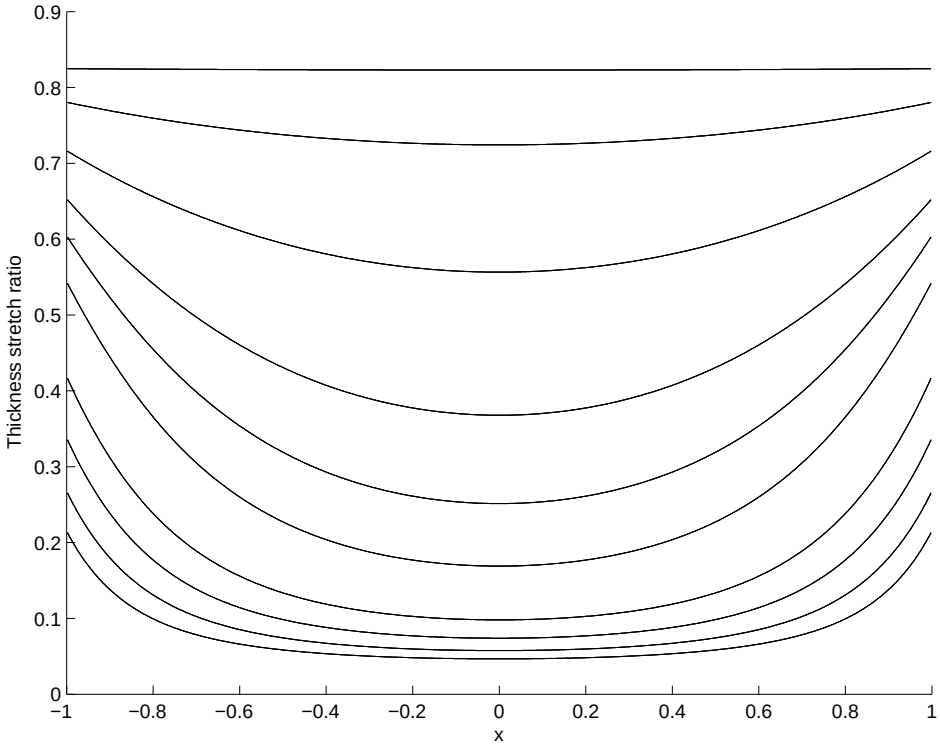

Figure 6.4: Thickness stretch ratios $\lambda_3 = 1/(\lambda_1\lambda_2)$ for the profiles of figure 6.1.

Table 6.1: In this table $P = 1$, we are estimating $J_1(\underline{U}) = -0.050397877719$, we use linear elements and we perform uniform refinement. The error behaves like $\mathcal{O}(h^2)$.

Elements m	Error est. $-a(\underline{u}_h, \hat{\underline{\psi}}_h)$	Asymptotic exactness $-a(\underline{u}_h, \hat{\underline{\psi}}_h)/(J_1(\underline{U}) - J_1(\underline{u}_h)) - 1$
8	-2.69×10^{-4}	-4.4×10^{-3}
16	-6.78×10^{-5}	-1.1×10^{-3}
32	-1.70×10^{-5}	-2.8×10^{-4}
64	-4.25×10^{-6}	-6.9×10^{-5}
128	-1.06×10^{-6}	-1.7×10^{-5}
256	-2.66×10^{-7}	-4.3×10^{-6}
512	-6.64×10^{-8}	-1.1×10^{-6}

Table 6.2: In this table $P = 1$, we are estimating $J_1(\underline{U})$, we use linear elements and we perform adaptive refinement. The accuracy desired corresponds to $\delta = 10^{-7}$.

Elements m	Error est. $-a(\underline{u}_h, \hat{\underline{\psi}}_h)$	Asymptotic exactness $-a(\underline{u}_h, \hat{\underline{\psi}}_h)/(J_1(\underline{U}) - J_1(\underline{u}_h)) - 1$
8	-2.69×10^{-4}	-4.4×10^{-3}
127	-1.06×10^{-6}	-1.7×10^{-5}
469	-6.68×10^{-8}	-8.6×10^{-7}

Table 6.3: In this table $P = 1$, we are estimating $J_1(\underline{U})$, we use quadratic elements and we perform uniform refinement. The error behaves like $\mathcal{O}(h^4)$.

Elements m	Error est. $-a(\underline{u}_h, \hat{\underline{\psi}}_h)$	Asymptotic exactness $-a(\underline{u}_h, \hat{\underline{\psi}}_h)/(J_1(\underline{U}) - J_1(\underline{u}_h)) - 1$
8	-1.74×10^{-7}	-4.0×10^{-4}
16	-1.10×10^{-8}	-1.0×10^{-4}
32	-6.88×10^{-10}	-2.5×10^{-5}
64	-4.30×10^{-11}	$+9.2 \times 10^{-6}$

Table 6.4: In this table $P = 1$, we are estimating $J_1(\underline{U})$, we use quadratic elements and we perform adaptive refinement. The accuracy desired corresponds to $\delta = 10^{-10}$.

Elements m	Error est. $-a(\underline{u}_h, \hat{\underline{\psi}}_h)$	Asymptotic exactness $-a(\underline{u}_h, \hat{\underline{\psi}}_h)/(J_1(\underline{U}) - J_1(\underline{u}_h)) - 1$
8	-1.74×10^{-7}	-4.0×10^{-4}
54	-6.09×10^{-11}	$+2.3 \times 10^{-6}$

Table 6.5: In this table $P = 1$, we are estimating $J_1(\underline{U})$, we use cubic elements and we perform uniform refinement.

Elements m	Error est. $-a(\underline{u}_h, \hat{\underline{\psi}}_h)$	Asymptotic exactness $-a(\underline{u}_h, \hat{\underline{\psi}}_h)/(J_1(\underline{U}) - J_1(\underline{u}_h)) - 1$
8	-2.69×10^{-11}	-9.0×10^{-4}

Table 6.6: In this table $P = 3$, we are estimating $J_1(\underline{U}) = -1.501627519302$, we use linear elements and we perform uniform refinement. The error behaves like $\mathcal{O}(h^2)$.

Elements m	Error est. $-a(\underline{u}_h, \hat{\underline{\psi}}_h)$	Asymptotic exactness $-a(\underline{u}_h, \hat{\underline{\psi}}_h)/(J_1(\underline{U}) - J_1(\underline{u}_h)) - 1$
8	-9.25×10^{-2}	-7.9×10^{-2}
16	-2.60×10^{-2}	-1.7×10^{-2}
32	-6.68×10^{-3}	-4.2×10^{-3}
64	-1.68×10^{-3}	-1.0×10^{-3}
128	-4.21×10^{-4}	-2.6×10^{-4}
256	-1.05×10^{-4}	-6.4×10^{-5}
512	-2.63×10^{-5}	-1.6×10^{-5}
1024	-6.58×10^{-6}	-3.8×10^{-6}
2048	-1.65×10^{-6}	-2.4×10^{-7}
4096	-4.12×10^{-7}	$+2.8 \times 10^{-6}$
8192	-1.03×10^{-7}	$+1.2 \times 10^{-5}$
16384	-2.57×10^{-8}	$+4.9 \times 10^{-5}$

Table 6.7: In this table $P = 3$, we are estimating $J_1(\underline{U})$, we use linear elements and we perform adaptive refinement. The accuracy desired corresponds to $\delta = 10^{-7}$.

Elements m	Error est. $-a(\underline{u}_h, \hat{\underline{\psi}}_h)$	Asymptotic exactness $-a(\underline{u}_h, \hat{\underline{\psi}}_h)/(J_1(\underline{U}) - J_1(\underline{u}_h)) - 1$
8	-9.25×10^{-2}	-7.9×10^{-2}
128	-4.21×10^{-4}	-2.6×10^{-4}
2030	-1.65×10^{-6}	-2.4×10^{-7}
9293	-7.02×10^{-8}	$+1.8 \times 10^{-5}$

Table 6.8: In this table $P = 3$, we are estimating $J_1(\underline{U})$, we use quadratic elements and we perform uniform refinement. The error behaves like $\mathcal{O}(h^4)$.

Elements m	Error est. $-a(\underline{u}_h, \hat{\underline{\psi}}_h)$	Asymptotic exactness $-a(\underline{u}_h, \hat{\underline{\psi}}_h)/(J_1(\underline{U}) - J_1(\underline{u}_h)) - 1$
8	-3.29×10^{-4}	-4.05×10^{-3}
16	-2.09×10^{-5}	-9.86×10^{-4}
32	-1.31×10^{-6}	-2.44×10^{-4}
64	-8.22×10^{-8}	-4.58×10^{-5}
128	-5.14×10^{-9}	$+2.30 \times 10^{-4}$
256	-3.21×10^{-10}	$+3.92 \times 10^{-3}$
512	-2.01×10^{-11}	$+6.68 \times 10^{-2}$

Table 6.9: In this table $P = 3$, we are estimating $J_1(\underline{U})$, we use quadratic elements and we perform adaptive refinement. The accuracy desired corresponds to $\delta = 10^{-10}$.

Elements m	Error est. $-a(\underline{u}_h, \hat{\underline{\psi}}_h)$	Asymptotic exactness $-a(\underline{u}_h, \hat{\underline{\psi}}_h)/(J_1(\underline{U}) - J_1(\underline{u}_h)) - 1$
8	-3.29×10^{-4}	-4.0×10^{-3}
128	-5.14×10^{-9}	$+2.3 \times 10^{-4}$
396	-4.06×10^{-11}	$+3.1 \times 10^{-2}$

Table 6.10: In this table $P = 3$, we are estimating $J_1(\underline{U})$, we use cubic elements and we perform uniform refinement. The error is consistent with $\mathcal{O}(h^6)$.

Elements m	Error est. $-a(\underline{u}_h, \hat{\underline{\psi}}_h)$	Asymptotic exactness $-a(\underline{u}_h, \hat{\underline{\psi}}_h)/(J_1(\underline{U}) - J_1(\underline{u}_h)) - 1$
8	-1.27×10^{-6}	-4.6×10^{-3}
16	-2.03×10^{-8}	-1.1×10^{-3}
32	-3.20×10^{-10}	$+3.6 \times 10^{-3}$
64	-5.01×10^{-12}	$+3.3 \times 10^{-1}$

Table 6.11: In this table $P = 3$, we are estimating $J_1(\underline{U})$, we use cubic elements and we perform adaptive refinement. The accuracy desired corresponds to $\delta = 10^{-10}$.

Elements m	Error est. $-a(\underline{u}_h, \hat{\underline{\psi}}_h)$	Asymptotic exactness $-a(\underline{u}_h, \hat{\underline{\psi}}_h)/(J_1(\underline{U}) - J_1(\underline{u}_h)) - 1$
8	-1.27×10^{-6}	-4.6×10^{-3}
37	-4.10×10^{-11}	$+3.2 \times 10^{-2}$

Table 6.12: In this table $P = 3$, we are estimating $J_2(\underline{U})$, we use linear elements and we perform uniform refinement. The error behaves like $\mathcal{O}(h^2)$.

Elements m	Error est. $-a(\underline{u}_h, \hat{\underline{\psi}}_h)$	Asymptotic exactness $-a(\underline{u}_h, \hat{\underline{\psi}}_h)/(J_2(\underline{U}) - J_2(\underline{u}_h)) - 1$
8	-1.46×10^{-3}	-1.0×10^{-1}
16	-4.12×10^{-4}	-2.1×10^{-2}
32	-1.06×10^{-4}	-5.1×10^{-3}
64	-2.67×10^{-5}	-1.3×10^{-3}
128	-6.70×10^{-6}	-3.2×10^{-4}
256	-1.68×10^{-6}	-7.9×10^{-5}
512	-4.19×10^{-7}	-1.9×10^{-5}
1024	-1.05×10^{-7}	-4.1×10^{-6}
2048	-2.62×10^{-8}	$+2.2 \times 10^{-6}$

Table 6.13: In this table $P = 3$, we are estimating $J_2(\underline{U}) = 0.046930267582$, we use linear elements and we perform adaptive refinement. The accuracy desired corresponds to $\delta = 10^{-7}$.

Elements m	Error est. $-a(\underline{u}_h, \hat{\underline{\psi}}_h)$	Asymptotic exactness $-a(\underline{u}_h, \hat{\underline{\psi}}_h)/(J_2(\underline{U}) - J_2(\underline{u}_h)) - 1$
8	-1.46×10^{-3}	-1.0×10^{-1}
128	-6.70×10^{-6}	-3.2×10^{-4}
1289	-4.52×10^{-8}	-7.1×10^{-5}

Table 6.14: In this table $P = 3$, we are estimating $J_2(\underline{U})$, we use quadratic elements and we perform uniform refinement. The error behaves like $\mathcal{O}(h^4)$.

Elements m	Error est. $-a(\underline{u}_h, \hat{\underline{\psi}}_h)$	Asymptotic exactness $-a(\underline{u}_h, \hat{\underline{\psi}}_h)/(J_2(\underline{U}) - J_2(\underline{u}_h)) - 1$
8	-2.11×10^{-5}	-2.3×10^{-3}
16	-1.39×10^{-6}	-5.2×10^{-4}
32	-8.82×10^{-8}	-1.2×10^{-4}
64	-5.54×10^{-9}	-1.5×10^{-5}
128	-3.47×10^{-10}	$+2.5 \times 10^{-4}$
256	-2.17×10^{-11}	$+4.1 \times 10^{-3}$

Table 6.15: In this table $P = 3$, we are estimating $J_2(\underline{U})$, we use quadratic elements and we perform adaptive refinement. The accuracy desired corresponds to $\delta = 10^{-10}$.

Elements m	Error est. $-a(\underline{u}_h, \hat{\underline{\psi}}_h)$	Asymptotic exactness $-a(\underline{u}_h, \hat{\underline{\psi}}_h)/(J_2(\underline{U}) - J_2(\underline{u}_h)) - 1$
8	-2.11×10^{-5}	-2.33×10^{-3}
128	-3.47×10^{-10}	$+2.5 \times 10^{-4}$
257	-1.79×10^{-11}	$+4.9 \times 10^{-3}$

Table 6.16: In this table $P = 3$, we are estimating $J_2(\underline{U})$, we use cubic elements and we perform uniform refinement. The error is consistent with $\mathcal{O}(h^6)$.

Elements m	Error est. $-a(\underline{u}_h, \hat{\underline{\psi}}_h)$	Asymptotic exactness $-a(\underline{u}_h, \hat{\underline{\psi}}_h)/(J_2(\underline{U}) - J_2(\underline{u}_h)) - 1$
8	-4.42×10^{-8}	-6.6×10^{-3}
16	-6.97×10^{-10}	-1.8×10^{-3}
32	-1.09×10^{-11}	$+7.7 \times 10^{-3}$

Table 6.17: In this table $P = 3$, we are estimating $J_2(\underline{U})$, we use cubic elements and we perform adaptive refinement. The accuracy desired corresponds to $\delta = 10^{-10}$.

Elements m	Error est. $-a(\underline{u}_h, \hat{\underline{\psi}}_h)$	Asymptotic exactness $-a(\underline{u}_h, \hat{\underline{\psi}}_h)/(J_2(\underline{U}) - J_2(\underline{u}_h)) - 1$
8	-4.42×10^{-8}	-6.6×10^{-3}
24	-1.21×10^{-11}	$+8.1 \times 10^{-3}$

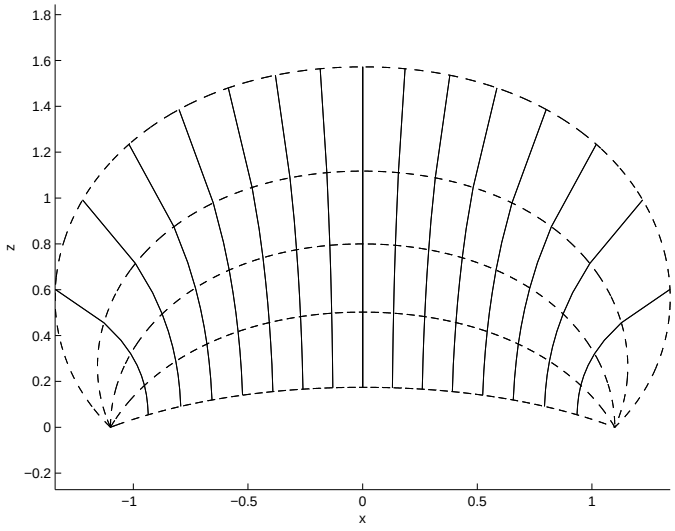

Figure 6.5: The deformed profiles and the material paths for the non-homogeneous sheet inflation.

Table 6.18: Adaptive refinements for the non-homogeneous sheet inflation using quadratic elements.

Elements	Error est.
8	-1.15×10^{-3}
106	-2.84×10^{-8}
299	-3.87×10^{-11}

Table 6.19: Uniform refinements for the non-homogeneous sheet inflation using quadratic elements.

Elements	Error est.
256	-1.78×10^{-9}
512	-1.11×10^{-10}
1024	-6.94×10^{-12}

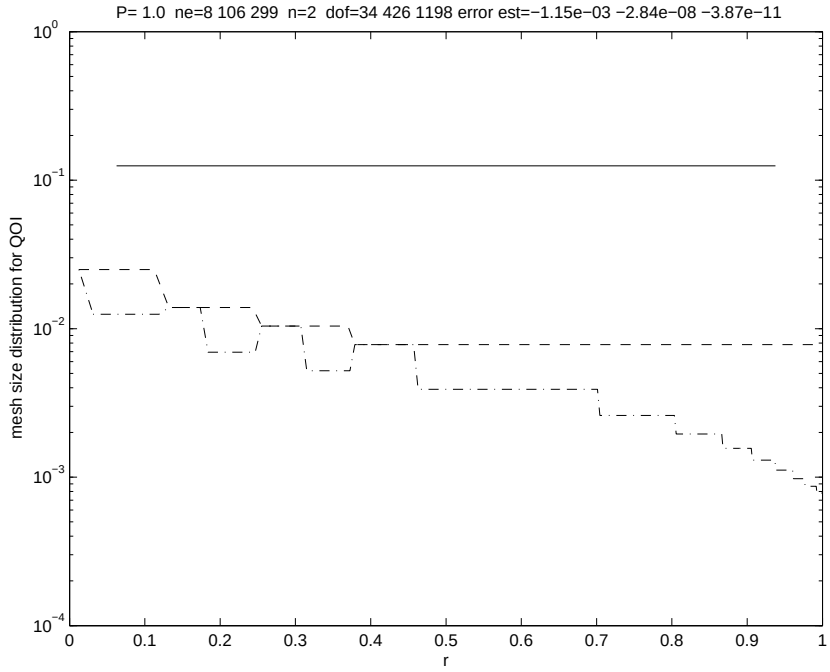

Figure 6.6: The variation of the mesh size for the meshes used in the results in table 6.18.

7 Results: modelling error

The graphs already shown in figure 6.1 give the deformed sheet profiles for different values of P/h_0 assuming that the hyperelastic membrane is deforming under quasi-static conditions, i.e. the deformed shape depends only on the current load and not on the loading history or the current rate at which the load is being applied. In particular the quasi-static assumption means that inertia terms can be ignored which is likely to be a valid approximation provided the inflation is not done too rapidly. An obvious modelling question is then 'how slow does the inflation process need to be for a given a quasi-static solution to be a good approximation to a solution obtained for a model in which the inertia term is included for a given QoI?'. A related question is 'how good is the estimate

$$J(\begin{pmatrix}\underline{U}\\ \underline{V}\end{pmatrix}) - J(\begin{pmatrix}\underline{u}_h\\ \underline{v}_h\end{pmatrix}) \approx F(\begin{pmatrix}\underline{\psi}_h\\ \underline{\theta}_h\end{pmatrix}) - A(\begin{pmatrix}\underline{u}_h\\ \underline{v}_h\end{pmatrix};\begin{pmatrix}\underline{\psi}_h\\ \underline{\theta}_h\end{pmatrix})?'. \tag{7.1}$$

For the axisymmetric inflation problem we are fortunate that it is not too computationally expensive to approximately solve the full dynamic problem to test the performance of the estimate although in other modelling situations this may be an expensive computation if a fine space mesh and a large number of time steps are required. It must of course not be overlooked that to obtain the error estimate we need to obtain $\underline{\psi}_h$ and $\underline{\theta}_h$ by solving a dual problem which, although linear, is a space time problem which may also need a fine mesh and a large number of time steps. To summarize the steps involved we do the following.

1. Solve the coarse problem to get $\underline{u}_h$ and $\underline{v}_h$.
2. Compute the estimate $J(\begin{pmatrix}\underline{u}_h\\ \underline{v}_h\end{pmatrix})$.
3. Solve the dual problem
$$A'(\begin{pmatrix}\underline{u}_h\\ \underline{v}_h\end{pmatrix};\begin{pmatrix}\underline{\alpha}\\ \underline{\beta}\end{pmatrix},\begin{pmatrix}\underline{\psi}_h\\ \underline{\theta}_h\end{pmatrix}) = J'(\begin{pmatrix}\underline{u}_h\\ \underline{v}_h\end{pmatrix};\begin{pmatrix}\underline{\alpha}\\ \underline{\beta}\end{pmatrix}), \quad \forall \begin{pmatrix}\underline{\alpha}\\ \underline{\beta}\end{pmatrix}.$$
4. Compute the error estimate $F(\begin{pmatrix}\underline{\psi}_h\\ \underline{\theta}_h\end{pmatrix}) - A(\begin{pmatrix}\underline{u}_h\\ \underline{v}_h\end{pmatrix};\begin{pmatrix}\underline{\psi}_h\\ \underline{\theta}_h\end{pmatrix})$.
5. Test the procedure, if possible, by attempting to approximate $\underline{U}_h$ and $\underline{V}_h$ by approximately solving the fine problem.

We consider the same inflation problem as in section 6 with the same material. The undeformed radius of the sheet is again 1, the initial thickness is taken as $h_0 = 10^{-2} = 0.01$ and the density of the incompressible material is taken as $\rho = 1$. Before the inflation is started we prestretch the sheet so that $U_1(1) = 0.1$, the sheet is then clamped at its edge and then a time dependent pressure $P(t)$ is applied where

$$P(t) = \frac{0.03t}{T}, \quad 0 \le t \le T. \tag{7.2}$$

The final pressure is thus $P(T) = 0.03$ so that $P(T)/h_0 = 3$ which corresponds to the largest forcing action used in figure 6.1 in the quasi-static inflation case. For the dynamic

problem we also need the initial velocity and this is set here as the velocity that the quasi-static solution gives at $t = 0$ so that there is no difference between the quasi-static and dynamic cases at this stage.

In the following we consider the deformation that is obtained at different final times T corresponding to the different values for the rate

$$r = \frac{0.03}{T} \tag{7.3}$$

for two different QoI. The rates that are considered are as follows: $r = 10^{-2}$, $r = 2 \times 10^{-2}$, $r = 3 \times 10^{-2}$, $\cdots$, $r = 9 \times 10^{-2}$, $r = 10 \times 10^{-2}$, $r = 20 \times 10^{-2}$, $r = 40 \times 10^{-2}$ and $r = 80 \times 10^{-2}$. The final deformation at these rates are shown in figure 7.1 and they show that there is a large difference between the profiles at the rates considered and hence there is a large difference between the final thickness (i.e. the thickness at time $t = T$) in these cases. We consider the following two quantities of interest concerned respectively with thickness and with kinetic energy.

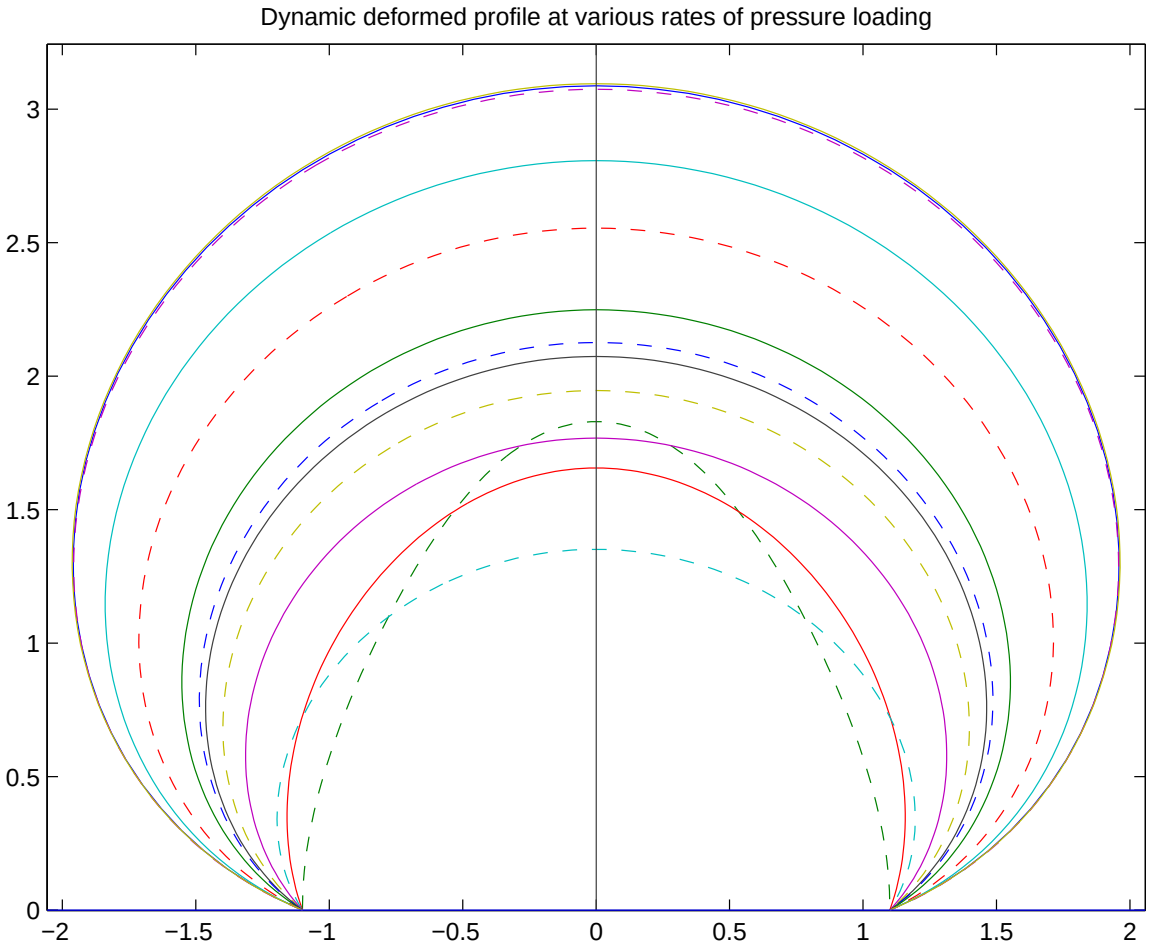

Figure 7.1: Deformation at final time $t = T$ when the pressure is 0.03 corresponding to the rates $r = 10^{-2}$, $r = 2 \times 10^{-2}$, $r = 3 \times 10^{-2}$, $\cdots$, $r = 9 \times 10^{-2}$, $r = 10 \times 10^{-2}$, $r = 20 \times 10^{-2}$, $r = 40 \times 10^{-2}$ and $r = 80 \times 10^{-2}$. The outermost curve is the slowest rate, the inner parabolic shaped curve is the fastest rate.

An average thickness near the pole at $t = T$

We take

$$J_3(\underline{U}) = \frac{1}{\delta}\int_0^b r\lambda_3(r,T)\,\mathrm{d}r, \quad \delta = \int_0^b r\,\mathrm{d}r, \quad b = 0.25 \text{ in the example,} \tag{7.4}$$

where recall that

$$\lambda_3 = \frac{1}{\lambda_1\lambda_2}, \quad \lambda_1^2 = (1+U_1')^2 + U_3'^2 \quad \text{and} \quad \lambda_2 = 1 + \frac{U_1}{r}.$$

The Gateaux derivative is straightforward to describe in this case in terms of quantities already given in this report. If we let $\lambda_1(s)$, $\lambda_2(s)$ and $\lambda_3(s)$ denote the stretch ratios corresponding to the displacement field $\underline{U} + s\underline{\alpha}$ then because $\lambda_3 = 1/(\lambda_1\lambda_2)$ we have, using the relations in equation (4.41),

$$\begin{aligned} \lambda_3'(\underline{U};\underline{\alpha}) &= \frac{\mathrm{d}}{\mathrm{d}s}\lambda_3(s)\bigg|_{s=0} = \frac{-1}{(\lambda_1\lambda_2)^2}\left(\lambda_1\left(\frac{\mathrm{d}\lambda_2}{\mathrm{d}s}\bigg|_{s=0}\right) + \left(\left(\frac{\mathrm{d}\lambda_1}{\mathrm{d}s}\bigg|_{s=0}\right)\lambda_2\right)\right. & (7.5)\\ &= -\lambda_3^2\left(\lambda_1\frac{\alpha_1}{r} + \lambda_2\left(\frac{1+U_1'}{\lambda_1}\alpha_1' + \frac{U_3'}{\lambda_1}\alpha_3'\right)\right). & (7.6) \end{aligned}$$

Thus

$$J'(\underline{U};\underline{\alpha}) = \int_0^b \left(\underline{\alpha}\cdot J_\alpha(t,T) + \underline{\alpha}'\cdot J_{\alpha'}(t,T)\right)\, r\mathrm{d}r \tag{7.7}$$

with

$$\underline{J}_\alpha(r,T) = -\frac{\lambda_3^2}{\delta}\begin{pmatrix}\lambda_1/r\\0\end{pmatrix}, \quad \underline{J}_{\alpha'}(r,T) = -\frac{\lambda_3^2\lambda_2}{\delta\lambda_1}\begin{pmatrix}1+U_1'\\U_3'\end{pmatrix}\bigg|_{t=T}. \tag{7.8}$$

A kinetic energy type term close to the pole and near the final time

Specifically we take

$$J_4(\underline{V}) = \frac{1}{2}\int_{0.9T}^T\int_0^b r\|\underline{V}\|^2\,\mathrm{d}r\mathrm{d}t, \quad \text{with } b = 0.25. \tag{7.9}$$

In this case the Gateaux derivative is simply

$$J_4'(\underline{V};\underline{\beta}) = \int_{0.9T}^T\int_0^b \underline{\beta}\cdot\underline{J}_\beta(r,t)\,r\mathrm{d}r\mathrm{d}t, \quad \text{where } \underline{J}_\beta(r,t) = \begin{pmatrix}V_1\\V_3\end{pmatrix}. \tag{7.10}$$

Numerical results

In table 7.1 we show the predictions for $J_3(\underline{U})$ corresponding to the different rates at which the pressure is applied. In this case the coarse solution prediction (i.e. the quasi-static solution prediction) is the same in each case and hence the error is the difference between each value and 0.0478. The error prediction is that obtained using the solution of the dual problem. When the rate is low the prediction and the actual error agree quite well (see the rate 1×10^{-2}) as the theory predicts whilst for the faster rates the prediction gives the correct order of magnitude but it is not a sharp estimate in this case. This is about as

much as can be expected as the theory only says that the estimate is good when the coarse solution is close to the fine problem. To get the error estimate we have to compute the dual solution which we find in this example is highly oscillatory in both space and time. Graphs of the profiles of ψ_1 and ψ_3 at the times T, $2T/3$, $T/3$ and 0 and corresponding to the fastest inflation rate are shown in figures 7.2, 7.3, 7.4 and 7.5. The final time value of $\underline{\psi}(r,T) = \underline{0}$ in this case but we have $\underline{\theta}(r,T) \neq \underline{0}$ because J_3 involves final time values. Similar profiles are obtained with all the other rates.

Table 7.1: The estimate of $J_3(\underline{U})$ by solving the fine problem, the error by predicting using the coarse problem and the estimate of the error computed using the dual solution.

Rate $\times 10^{-2}$	Estimate	Error	Error Prediction
0	4.782×10^{-2}	-	-
1	4.767×10^{-2}	-1.477×10^{-4}	-1.406×10^{-4}
2	4.782×10^{-2}	7.329×10^{-6}	-1.956×10^{-4}
3	5.323×10^{-2}	5.409×10^{-3}	3.647×10^{-3}
4	6.070×10^{-2}	1.288×10^{-2}	8.168×10^{-3}
5	7.405×10^{-2}	2.623×10^{-2}	1.338×10^{-2}
10	1.438×10^{-1}	9.605×10^{-2}	3.127×10^{-2}
20	1.775×10^{-1}	1.297×10^{-1}	4.217×10^{-2}
40	2.270×10^{-1}	1.792×10^{-1}	4.819×10^{-2}
80	4.399×10^{-1}	3.921×10^{-1}	6.511×10^{-2}

In table 7.2 we show the predictions for $J_4(\underline{V})$ obtained by solving the fine problem, obtained by just solving the coarse problem (i.e. solving the quasi-static problem for the displacement and then recovering the velocity) together with the actual error and the prediction of the error. In this case the error prediction is quite good throughout even when the error is large. The good prediction throughout seems to be connected to a dual solution which is 'fairly simple' in that it is not highly oscillatory in space or time. In figures 7.6, 7.7, 7.8 and 7.9 we show graphs of the profiles of ψ_1 and ψ_3 at the times T, $2T/3$, $T/3$ and 0 respectively. In this case as $J_4(\underline{V})$ does not involve final time values we have $\underline{\psi}(r,T) = \underline{\theta}(r,T) = \underline{0}$, $0 \leq r \leq 1$.

In all the computations given the coarse solution was obtained using $\tilde{M} = 20$ quadratic elements and $N = 200$ time steps. The dual solution was obtained with 40 quadratic elements and 400 time steps. This seems to be enough (and possibly more than enough) to ensure that the numbers given in the tables here are about accurate to all the digits given. To support this claim we give in table 7.3 values for the actual error and the prediction of this error for the inflation rate of 4×10^{-2} obtained using a different number of space elements and a different number of time steps. The closeness of the numbers in each column suggests that the space and time meshes are fine enough and that the error in estimating the QoI in each case is predominantly just the modelling error. The smoothness of the deformed profiles in figure 7.1 and also the results in table 7.2 indicate that not too many quadratic elements are needed for high accuracy but that a much larger number of time steps are needed to get a sufficiently accurate solution to the fine problem and indeed to the dual problem in some cases (e.g. the case of predicting $J_3(\underline{U})$).

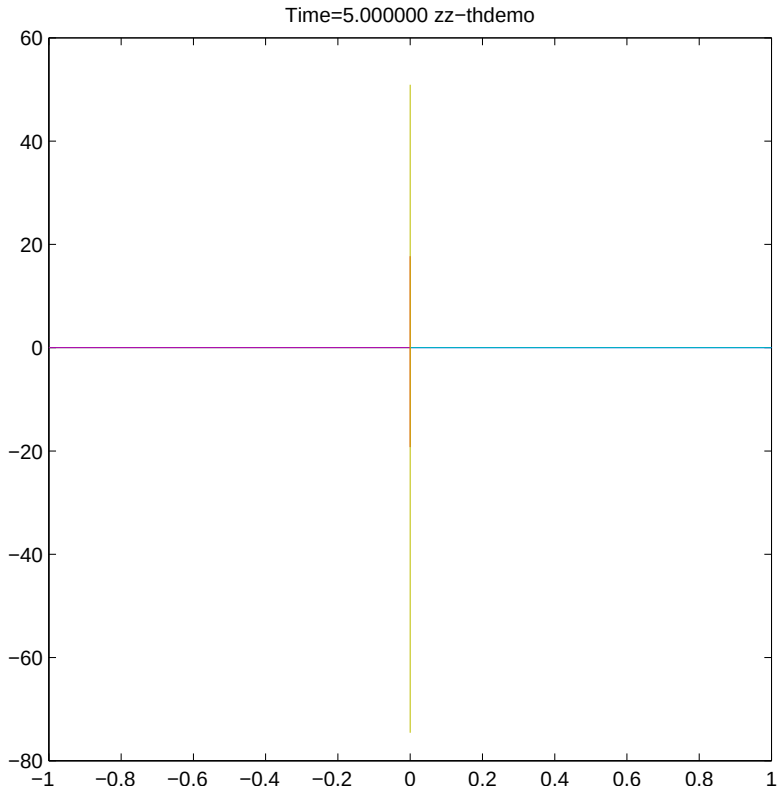

Figure 7.2: Graphs of $\psi_1(.,T)$ and $\psi_3(.,T)$ at the fastest rate. Both are 0.

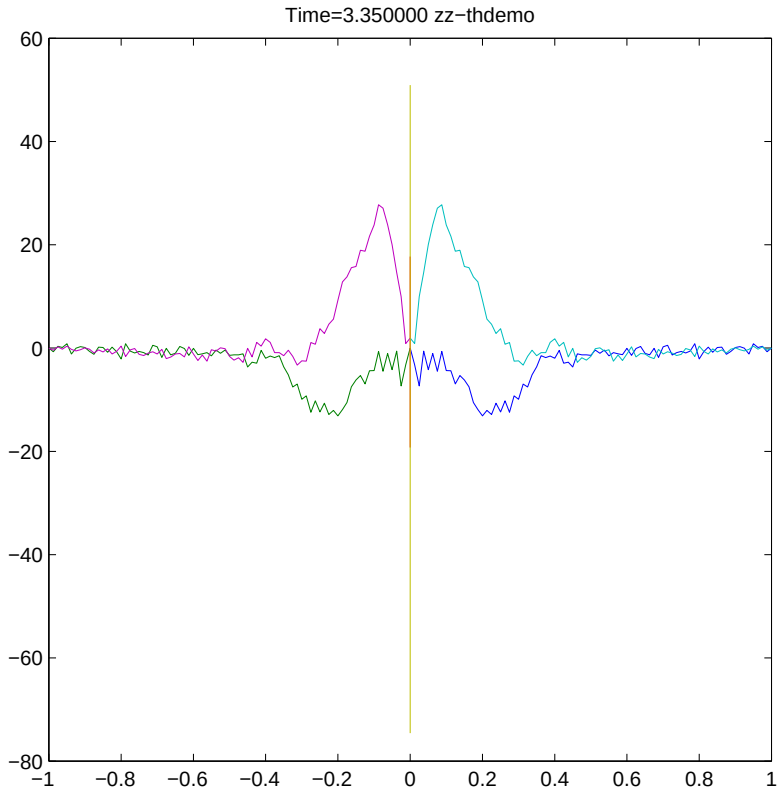

Figure 7.3: Graphs of $\psi_1(.,2T/3)$ and $\psi_3(.,2T/3)$ at the fastest rate.

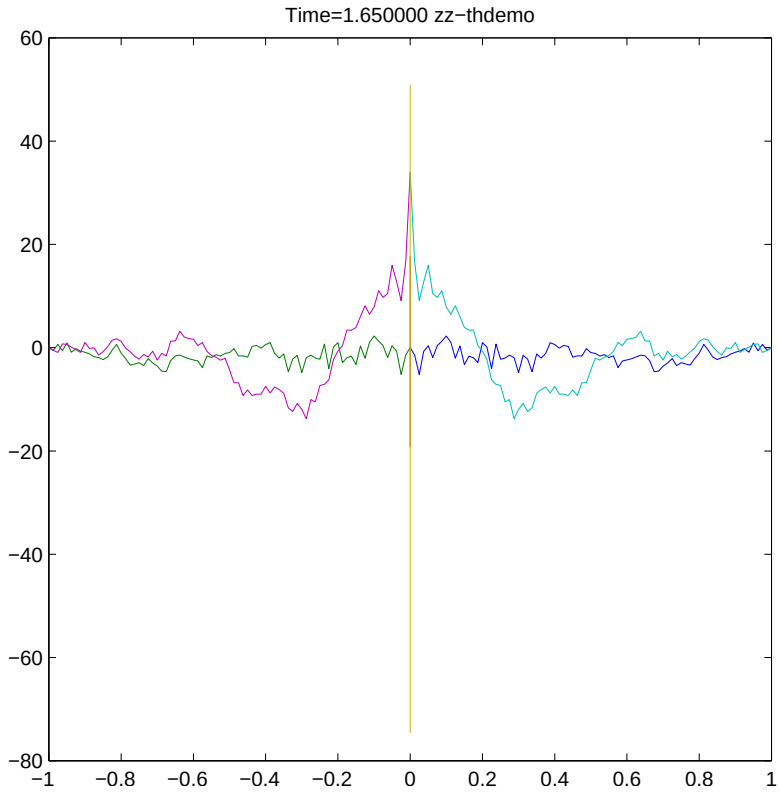

Figure 7.4: Graphs of $\psi_1(.,T/3)$ and $\psi_3(.,T/3)$ at the fastest rate.

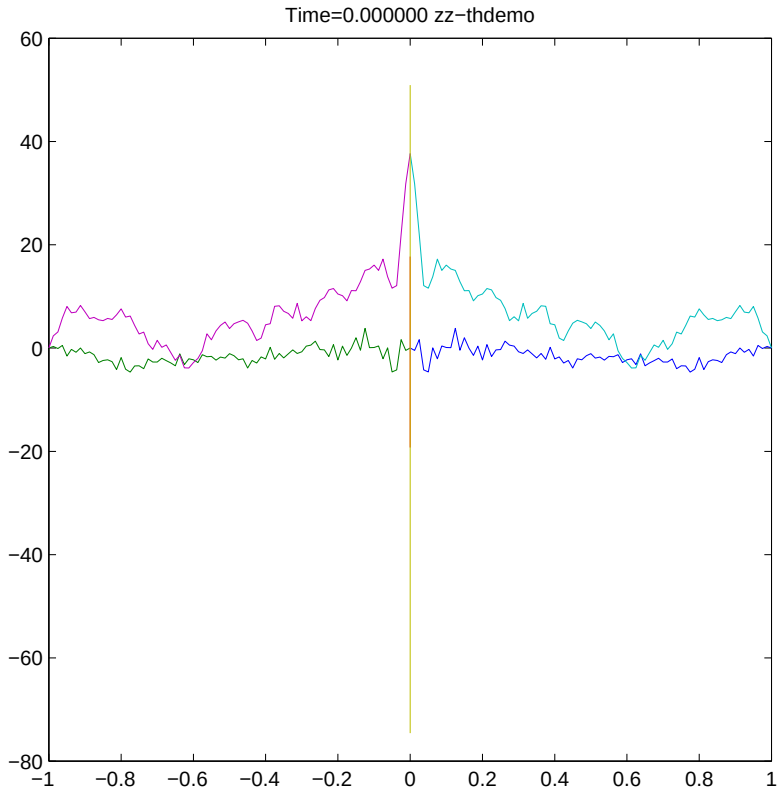

Figure 7.5: Graphs of $\psi_1(.,0)$ and $\psi_3(.,0)$ at the fastest rate.

Table 7.2: Prediction of $J_4(\underline{V})$ by solving the fine problem, by solving the coarse problem, the error in the prediction and the estimate of the error by solving obtained using the solution to the dual problem.

Rate $\times 10^{-2}$	Exact	Estimate	Error	Error Prediction
1	4.04×10^{-2}	4.37×10^{-2}	3.32×10^{-3}	3.10×10^{-3}
2	8.07×10^{-2}	1.02×10^{-1}	2.10×10^{-2}	1.94×10^{-2}
3	1.21×10^{-1}	1.19×10^{-1}	-2.45×10^{-3}	4.03×10^{-3}
4	1.61×10^{-1}	1.02×10^{-1}	-5.98×10^{-2}	-5.33×10^{-2}
5	2.02×10^{-1}	8.12×10^{-2}	-1.21×10^{-1}	-1.23×10^{-1}
10	4.03×10^{-1}	4.53×10^{-2}	-3.58×10^{-1}	-4.98×10^{-1}
20	8.07×10^{-1}	1.12×10^{-2}	-7.96×10^{-1}	$-1.40\times10^{+0}$
40	$1.61\times10^{+0}$	2.74×10^{-2}	$-1.59\times10^{+0}$	$-2.81\times10^{+0}$
80	$3.23\times10^{+0}$	5.74×10^{-2}	$-3.17\times10^{+0}$	$-5.66\times10^{+0}$

Table 7.3: The 'actual error' and the prediction of the error using the dual solution using different numbers of quadratic space elements and time steps in the case of the inflation rate of 4×10^{-2}.

		Thickness QoI		K.E. QoI	
ne	nt	Actual error	Prediction	Actual error	prediction
20	100	1.284×10^{-2}	7.783×10^{-3}	-5.960×10^{-2}	-5.440×10^{-2}
20	200	1.287×10^{-2}	8.165×10^{-3}	-5.971×10^{-2}	-5.324×10^{-2}
40	200	1.287×10^{-2}	8.165×10^{-3}	-5.974×10^{-2}	-5.326×10^{-2}
40	400	1.289×10^{-2}	8.169×10^{-3}	-5.976×10^{-2}	-5.329×10^{-2}

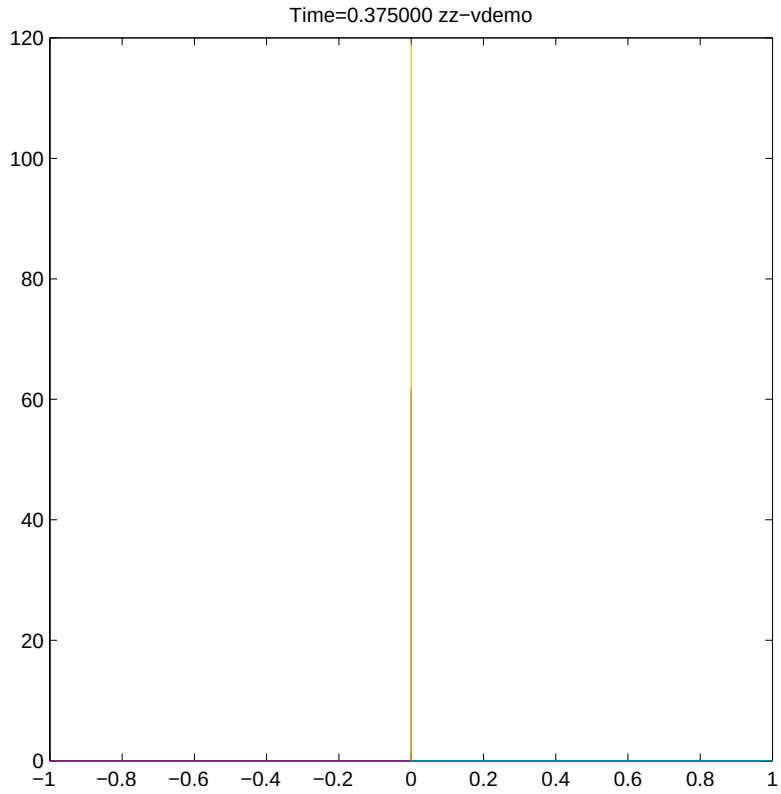

Figure 7.6: Graphs of $\psi_1(.,T)$ and $\psi_3(.,T)$ at the fastest rate. Both are 0.

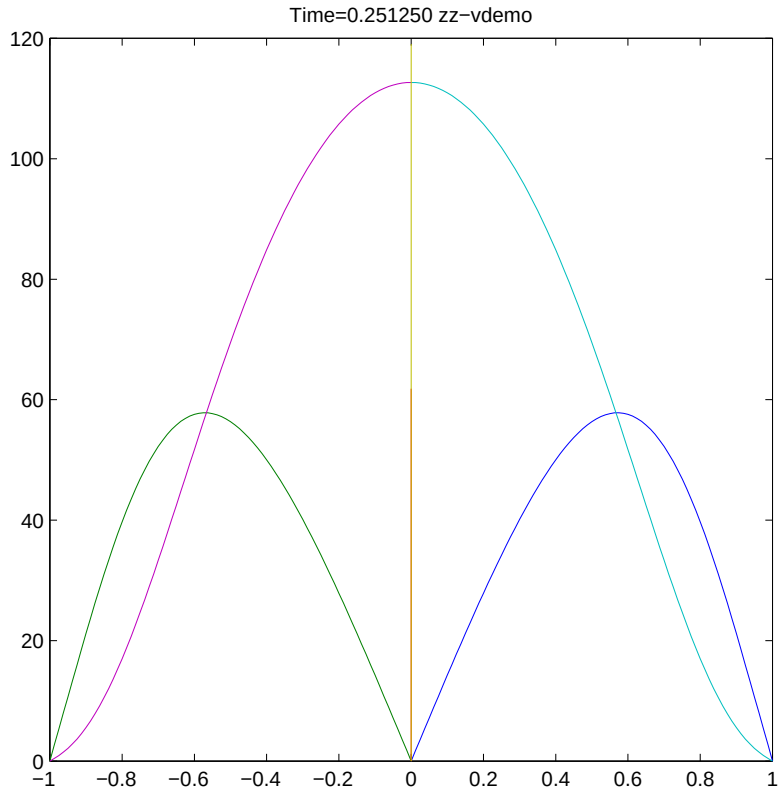

Figure 7.7: Graphs of $\psi_1(.,2T/3)$ and $\psi_3(.,2T/3)$ at the fastest rate.

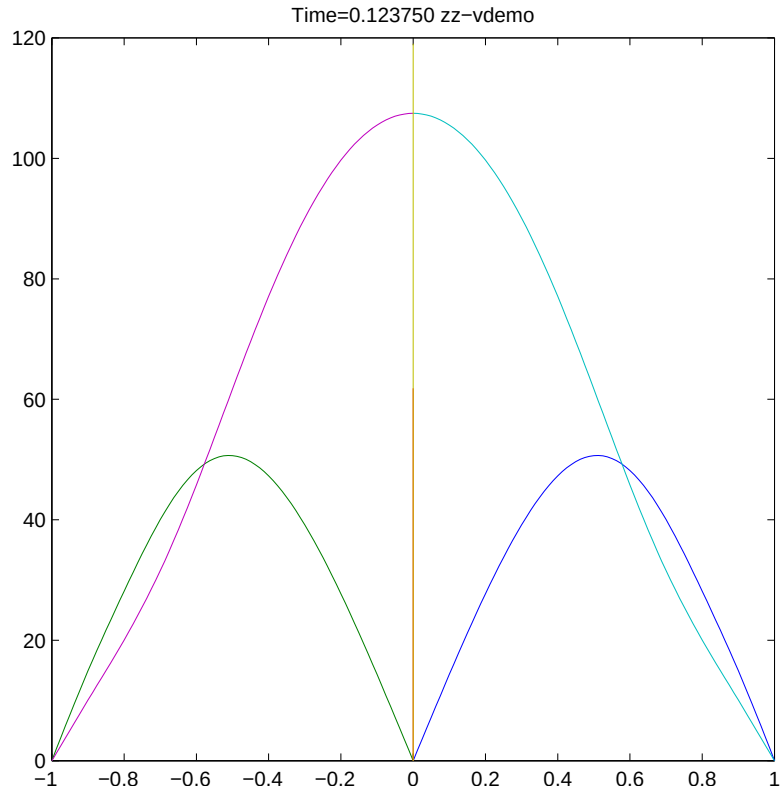

Figure 7.8: Graphs of $\psi_1(.,T/3)$ and $\psi_3(.,T/3)$ at the fastest rate.

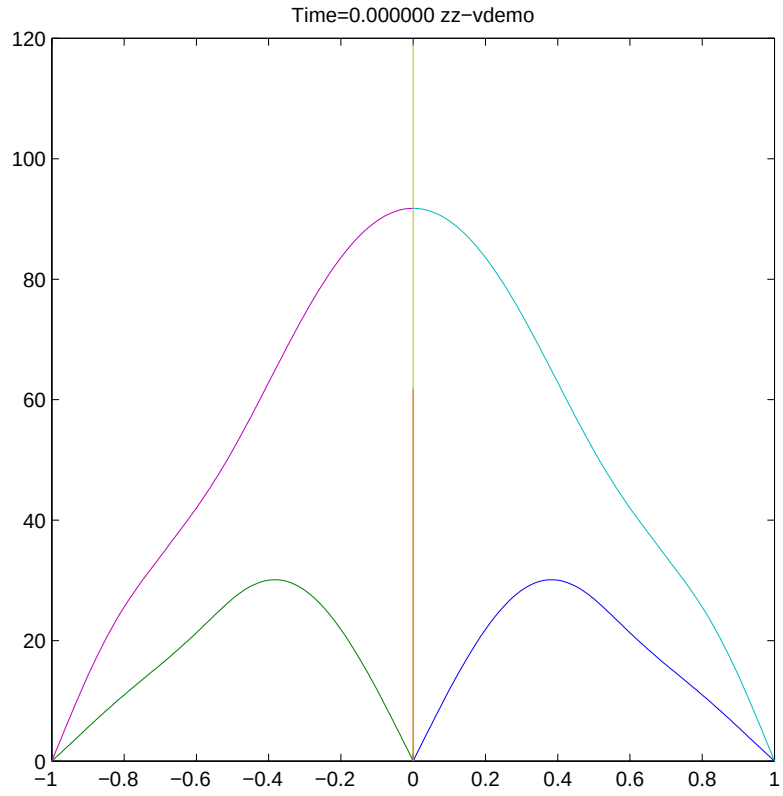

Figure 7.9: Graphs of $\psi_1(.,0)$ and $\psi_3(.,0)$ at the fastest rate.

8 Conclusions

Computer simulations are an indispensable tool in modern engineering research and design. They are used to create virtual components which can then be subjected to virtual operating environments. The components can be altered with respect to geometry, configuration and constitution and the simulation re-virtualised in either the same or a modified virtual environment. The cost of simulations *in silico* is typically trivial compared with that of building hardware prototypes and simulating their in-service actuality in a laboratory.

The main drawback with virtual experiments is the issue of reliability: the uncertainty associated with how closely the output matches that which would be obtained in the real world. When simulating in the virtual world the engineer usually has in mind some Quantity of Interest (QoI), and it is the reliable and accurate determination of this quantity that forms the goal of the computation. There are two principal reasons why the virtually realised QoI might not match that which would be observed in the real world.

Modelling error: this occurs when the physics of a very difficult underlying problem are approximated by those of a simpler problem (e.g. the approximation of a highly heterogeneous 3D body by a homogenised 2D cross section). It is common to talk of approximating a fine problem by a coarse problem, but one should not be led into believing that the coarse problem is necessarily in any sense easy. Indeed, the entire field of mathematical modelling is, by its nature, laden with modelling errors and yet still contains many forbidding problems.

Discretization error: the more manageable coarser problem can only be virtualised with the aid of discretization techniques (e.g. finite element methods). These generate discretization errors which can be controlled and diminished by suitable enrichment techniques (e.g. mesh refinement).

Methods for quantifying and controlling the second type of error have been studied by numerical analysts for many years and although for a wide class of problems and error measures, they can be said to be well understood, the estimation of error in QoI's is a young subject.

On the other hand, methods of quantifying and controlling the first type of error are only partially understood for a small class of problems. It is a major challenge in modern applied computational mathematics to devise theories, algorithms and software that, for any given virtualisation, can provide *a posteriori* a quantitative assessment of the size of these errors relative to the engineer's QoI, and possibly adapt the virtual world in an intelligent and automatic way so as to reduce these errors to an acceptable level.

In this project we have applied state-of-the-art mathematical theory to a practical engineering problem in membrane inflation. We have applied modern methods of *a posteriori* error estimation in order to address the error in engineering quantities of interest that arise from modelling simplifications and also from finite element approximation. Our results show that this technique works in that it can be used to adaptively optimise the finite element mesh, as well as give an indication of the physical error contained in the modelling assumptions.

The eventual benefit of research of this nature and the downstream uptake of the techniques and methodology into commercial engineering software cannot be overstated. By isolating and estimating the two principal sources of error in physical simulations (modelling and discretization) the software will allow the practitioner to assign a degree of confidence in the results that has never before been possible.

However, what is absolutely clear from our efforts thus far is that to make further progress in research of this nature some form of 'computational workhorse' is needed. So far, as is common in primary research, we have generated our own software using, where possible, codes from earlier efforts. This approach has certain advantages in terms of code control and ownership, but has severe disadvantages in terms of the time it takes to bring a theoretical result to practical fruition.

9 Appendix: Some of the notation

X_1, X_2, X_3	Cartesian coordinates. Typically upper case letter are used when we consider the undeformed position of a point.
x_1, x_2, x_3	Cartesian coordinates. Typically lower case letter are used when we consider the deformed position of a point.
r, ψ, X_3	Cylindrical polar coordinates, r is the radius, ψ is the angle and X_3 is the vertical coordinate.
$\underline{e}_1$, $\underline{e}_2$, $\underline{e}_3$,	These denote the cartesian base vectors when cartesian coordinates are being considered.
$\underline{e}_r$, $\underline{e}_\psi$, $\underline{e}_3$,	These denote the base vectors when cylindrical polars are being considered.
t	t denotes time when space-time problems are considered.
Ω_{3D}	The region of a general three-dimensional body when it is undeformed.
Ω	The region of the undeformed mid-surface of the membrane.
T	The final time.
Q	This is used for the space time region $Q = \Omega \times (0, T)$.
$'$	When a function only depends on one variable this is used to denote the derivative with respect to that variable. This is extensively used in axi-symmetric problems when we have quantities which only depend on r.
$''$	The second derivative of a function of one variable. Similarly $'''$ denotes the third derivative etc..
$\dot{}$	The first time derivative.
$\ddot{}$	The second time derivatives.
$\underline{U}$	The exact displacement. When cartesian coordinates are being used $\underline{U} = (U_1, U_2, U_3)^T$ with U_i denoting the component in the $\underline{e}_i$ direction. When cylindrical polar coordinates are being used and axi-symmetric deformations are being considered we let $\underline{U} = (U_1, U_3)^T$ with U_1 denoting the component in the $\underline{e}_r$ direction and with U_3 denoting the component in the $\underline{e}_3$ direction.
$\underline{u}$	An approximate displacement. When cartesian coordinates are being used $\underline{u} = (u_1, u_2, u_3)^T$ with u_i denoting the component in the $\underline{e}_i$ direction. When cylindrical polar coordinates are being used and axi-symmetric deformations are being considered we let $\underline{u} = (u_1, u_3)^T$ with u_1 denoting the component in the $\underline{e}_r$ direction and with u_3 denoting the component in the $\underline{e}_3$ direction.
$\underline{V}$	The exact velocity. In the application we enforce, weakly, the condition $\underline{V} = \dot{\underline{U}}$. When cylindrical polar coordinates are being used and axi-symmetric deformations are being considered we let $\underline{V} = (V_1, V_3)^T$ with W_1 denoting the component in the $\underline{e}_r$ direction and with W_3 denoting the component in the $\underline{e}_3$ direction.
$\underline{v}$	An approximate velocity. When cylindrical polar coordinates are being used and axi-symmetric deformations are being considered we let $\underline{v} = (v_1, v_3)^T$ with v_1 denoting the component in the $\underline{e}_r$ direction and with v_3 denoting the component in the $\underline{e}_3$ direction.
V	In the abstract formulation V denotes a function space.

$J(.)$ The quantity of interest (QoI). This will typically depend on the displacement and/or the velocity and/or the first spatial derivatives of these.

ρ The density of the material.

h_0 The undeformed thickness of a sheet.

P The applied pressure. Typically we have $P = P(t)$.

∇_{3D} The gradient operator in the fully three-dimensional case.

$$\nabla_{3D}\underline{U} = \left(\frac{\partial \underline{U}}{\partial X_1}, \frac{\partial \underline{U}}{\partial X_2}, \frac{\partial \underline{U}}{\partial X_3}\right).$$

∇ The gradient operator in the membrane case. When the membrane model is being considered $\nabla\underline{U}$ means the 3×2 tensor

$$\nabla\underline{U} = \left(\frac{\partial \underline{U}}{\partial X_1}, \frac{\partial \underline{U}}{\partial X_2}\right).$$

Div The divergence operator with respect to X_1, X_2 and X_3. In the context when equations of motion and/or quasi-static equilibrium are being described and we have the fully three dimensional case, the divergence of $\mathbf{\Pi}_{3D}$ is the vector

$$\text{Div}\,\mathbf{\Pi}_{3D} = \begin{pmatrix} \frac{\partial \Pi_{11}}{\partial X_1} + \frac{\partial \Pi_{21}}{\partial X_2} + \frac{\partial \Pi_{31}}{\partial X_3} \\ \frac{\partial \Pi_{12}}{\partial X_1} + \frac{\partial \Pi_{22}}{\partial X_2} + \frac{\partial \Pi_{32}}{\partial X_3} \\ \frac{\partial \Pi_{13}}{\partial X_1} + \frac{\partial \Pi_{23}}{\partial X_2} + \frac{\partial \Pi_{33}}{\partial X_3} \end{pmatrix}$$

$\mathbf{I}_{3D}$, $\mathbf{I}$ Identity tensors

$$\mathbf{I}_{3D} = \begin{pmatrix} 1 & 0 & 0 \\ 0 & 1 & 0 \\ 0 & 0 & 1 \end{pmatrix}, \quad \mathbf{I} = \begin{pmatrix} 1 & 0 \\ 0 & 1 \\ 0 & 0 \end{pmatrix}.$$

$\mathbf{F}_{3D}$ The 3×3 deformation gradient when a fully three dimensional deformation is being considered. It is the Jacobian matrix of the mapping $\underline{X} \to \underline{x} = \underline{X} + \underline{U}$ and is given by $\mathbf{F}_{3D} = \mathbf{I}_{3D} + \nabla\underline{U}$.

$\mathbf{F}$ The 3×2 membrane deformation gradient. In the membrane model application this is the first two columns of $\mathbf{F}_{3D}$.

λ_1, λ_2, λ_3 The principal stretch ratios, i.e. λ_i^2, $i = 1, 2, 3$, are the eigenvalues of $\mathbf{F}_{3D}^T\mathbf{F}_{3D}$ and of $\mathbf{F}_{3D}\mathbf{F}_{3D}^T$ in the fully three-dimensional case. In the membrane case λ_i^2, $i = 1, 2$, are the eigenvalues of $\mathbf{F}^T\mathbf{F}$ and correspond to stretching in directions tangential to the mid-surface. In the incompressible membrane case we have $\lambda_3 = 1/(\lambda_1\lambda_2)$.

W The strain energy function of a hyperelastic material. In the case of incompressible membrane models we have $W = W(\lambda_1, \lambda_2)$.

$\boldsymbol{\sigma}$ The 3×3 Cauchy stress tensor. This is symmetric.

$\mathbf{\Pi}_{3D}$ The 3×3 nominal stress tensor. This is not in general symmetric and it is related to $\boldsymbol{\sigma}$ by the relation $\mathbf{\Pi}_{3D} = (\det \mathbf{F}_{3D})\mathbf{F}_{3D}^{-1}\boldsymbol{\sigma}$.

$\mathbf{\Pi}$ — The 2×3 nominal stress tensor in the membrane model. As a consequence of the membrane simplification this is the first two rows of $\mathbf{\Pi}_{3D}$.

$\mathbf{\Pi}^T$ — The 3×2 first Piola stress tensor in the membrane model.

: — The double dot product operation, i.e. for tensors $\mathbf{A}$ and $\mathbf{B}$ of compatible sizes we have $\mathbf{A} : \mathbf{B} = \sum_{ij} A_{ij} B_{ij} = \text{tr}(\mathbf{A}^T \mathbf{B})$.

$a(.;.)$ — The form used in the description of the quasi-static problem. The semi-colon indicates that the functional is non-linear in the term before the semi-colon and is linear in the term afterwards.

$A(.;.)$ — The form used in the abstract description and also the form used for the weak form of the dynamic problem.

$\tilde{a}(.;.)$ — In the formulations this is used for the integrand or part of the integrand in the expressions for $a(.;.)$ and/or for $A(.;.)$.

$F(.)$ — A linear functional appearing on the right hand side in expressions such as $a(\underline{U};\underline{\psi}) = F(\underline{\psi})$ or $A(\begin{pmatrix}\underline{U}\\ \underline{V}\end{pmatrix};\begin{pmatrix}\underline{\psi}\\ \underline{\theta}\end{pmatrix}) = F(\begin{pmatrix}\underline{\psi}\\ \underline{\theta}\end{pmatrix})$ where $\underline{\psi}$ and $\underline{\theta}$ are test vectors.

$a'(.;.,.)$, $A'(.;.,.)$ — The first Gateaux derivatives of a and A with, for example,

$$\begin{aligned} a'(\underline{U};\underline{\alpha},\underline{\psi}) &= \frac{\mathrm{d}}{\mathrm{d}s} a(\underline{U}+s\underline{\alpha};\underline{\psi})\Big|_{s=0}, \\ A'(\begin{pmatrix}\underline{U}\\ \underline{V}\end{pmatrix};\begin{pmatrix}\underline{\alpha}\\ \underline{\beta}\end{pmatrix},\begin{pmatrix}\underline{\psi}\\ \underline{\theta}\end{pmatrix}) &= \frac{\mathrm{d}}{\mathrm{d}s} A(\begin{pmatrix}\underline{U}\\ \underline{V}\end{pmatrix}+s\begin{pmatrix}\underline{\alpha}\\ \underline{\beta}\end{pmatrix};\begin{pmatrix}\underline{\psi}\\ \underline{\theta}\end{pmatrix})\Big|_{s=0}. \end{aligned}$$

The term just to the right of the semi-colon indicates the "direction" in which we differentiate. Higher derivatives are similarly defined.

$F'(.;.)$ — The first Gateaux derivative of F. $F'(\underline{U};\underline{\psi})$ means

$$F'(\underline{U};\underline{\psi}) = \frac{\mathrm{d}}{\mathrm{d}s} F(\underline{U}+s\underline{\psi})\Big|_{s=0}.$$

Higher derivatives are similarly defined.

$\begin{pmatrix}\underline{U}\\ \underline{V}\end{pmatrix}$ — The unknown displacement and velocity in the dynamic problem.

$\begin{pmatrix}\underline{\psi}\\ \underline{\theta}\end{pmatrix}$ — The test vector in the dynamic problem and the unknown vector in the dual problem.

$\begin{pmatrix}\underline{\alpha}\\ \underline{\beta}\end{pmatrix}$ — The test vector in the dual problem.

$L_2((\Omega)$ — The space of functions which are square integrable over the domain Ω.

$H^1(\Omega)$ — The space of functions whose first weak derivatives are square integrable over the domain Ω.

$H^1((0,T),H^1(\Omega))$ — $u_i(\underline{x},t)$ is in this space if $u_i(.,t) \in H^1(\Omega)$ for each time $t \in (0,T)$ and $u_i(\underline{x},.) \in H^1(0,T)$ for each point $\underline{x} \in \Omega$.

$H^1((0,T),L_2(\Omega))$ — $v_i(\underline{x},t)$ is in this space if $v_i(.,t) \in L_2(\Omega)$ for each time $t \in (0,T)$ and $v_i(\underline{x},.) \in H^1(0,T)$ for each point $\underline{x} \in \Omega$.

$L_2((0,T),H^1(\Omega))$ — $\psi_i(\underline{x},t)$ is in this space if $\psi_i(.,t) \in H^1(\Omega)$ for each time $t \in (0,T)$ and $\psi_i(\underline{x},.) \in L_2(0,T)$ for each point $\underline{x} \in \Omega$.

$L_2((0,T),L_2(\Omega))$	$\theta_i(\underline{x},t)$ is in this space if $\theta_i(.,t) \in L_2(\Omega)$ for each time $t \in (0,T)$ and $\theta_i(\underline{x},.) \in L_2(0,T)$ for each point $\underline{x} \in \Omega$.

References

[1] Wolfgang Bangerth and Rolf Rannacher. Finite element approximation of the acoustic wave equation: Error estimation and mesh adaptation. *East-West Journal of Numerical Mathematics*, (4):263–282, 1999.

[2] R Becker and R Rannacher. An optimal control approach to a posteriori error estimation in finite element methods. Technical report, 2001. `www.iwr.uni-heidelberg.de/organization/sfb359/PP/Preprint2001-14.ps.gz`.

[3] J. T. Oden and S. Prudhomme. Adaptive modeling in computational mechanics. Technical report, Technical Report 02-05, TICAM, University of Texas at Austin, 2002. `www.ices.utexas.edu/research/reports/2002/0205.pdf`.